Local Metabolism of Ethanol to Acetic Acid/Acetate in the Central Nucleus of Amygdala Elicits Sympathoexcitatory Responses through Activation of NMDAR in Sprague Dawley Rats

Andrew D. Chapp[1,2,3*], Michael J. Huber[1,2], Andréa R. Collins[4], Kyle M. Driscoll[2], Jessica E. Behnke[1,2], Robert A. Larson[1,2], Zhiying Shan[1,2], Li. Zhang[5], Qing-Hui Chen[1,2*]

Affiliations:

[1]Department of Kinesiology and Integrative Physiology, Michigan Technological University, Houghton, MI 49931

[2]Department of Biological Sciences, Michigan Technological University, Houghton, MI 49931

[3]Department of Neuroscience, University of Minnesota, Minneapolis, MN 55455

[4]Department of Psychiatry, University of California San Francisco, Fresno, CA 93701

[5]Laboratory for Integrative Neuroscience, National Institute on Alcohol Abuse and Alcoholism, National Institutes of Health, Rockville, MD 20852

Running Title: Acetate activates NMDAR in the CeA

Word Count:

Word Count: 10,138

Figures: 9

Graphical Figure: 1

Tables: 1

*Correspondence to:

Qing-Hui Chen, Ph.D.

Department of Kinesiology and Integrative Physiology,
Michigan Technological University.
SDC, 1400 Townsend Drive, Houghton, MI 49931
Phone: (906) 487-1629; FAX: (906) 487-0985
Email:qinghuic@mtu.edu

Andrew D. Chapp, Ph.D.
Department of Neuroscience
University of Minnesota-Twin Cities
321 Church St SE, Minneapolis, MN 55455
Email: achapp@umn.edu

ABSTRACT

Binge alcohol consumption elicits robust sympathoexcitation and excitatory neuronal output. However, the central mechanism that mediates these effects remains elusive. We investigated the effects of ethanol metabolism within the central nucleus of the amygdala (CeA) on sympathoexcitation, and elucidated the role of acetate in these excitatory responses. *In vivo* arterial blood pressure, heart rate and sympathetic nerve activity responses to CeA microinjected ethanol or acetate with appropriate inhibitors/antagonists were tracked. *In vitro* whole-cell electrophysiology recording responses to acetate in CeA neurons with axon projecting to the rostral ventrolateral medulla (CeA-RVLM) were investigated, and cytosolic calcium responses in primary neuronal cultures were quantified. We demonstrate that in Sprague Dawley rats, local brain metabolism of ethanol in the CeA to acetic acid/acetate elicits sympathoexcitatory responses *in vivo* through activation of NMDA receptor (NMDAR). Alcohol dehydrogenase or aldehyde dehydrogenase inhibition using fomepizole or cyanamide and NMDAR antagonism using AP5 or memantine blunted these effects. Whole-cell patch-clamp recordings in brain slices containing autonomic CeA-RVLM neurons revealed a dose-dependent increase in neuronal excitability in response to acetate. NMDAR antagonists suppressed the acetate-induced increase in CeA-RVLM neuronal excitability, and memantine suppressed the direct activation of NMDAR-mediated inward currents by acetate in brain slices. We observed that acetate increased cytosolic Ca^{2+} in a time-dependent manner in primary neuronal cell cultures. The acetate enhancement of calcium signaling was abolished by memantine. These findings suggest that within the CeA, ethanol is sympathoexcitatory through local brain metabolism, which generates acetic acid/acetate leading to activation of NMDAR.

26 **NEW AND NOTEWORTHY:**

27 Brain ethanol metabolism to acetic acid (vinegar)/acetate causes activation of N-methyl-
28 D-aspartate receptors (NMDARs) in the central nucleus of the amygdala and elicits
29 sympathoexcitatory responses. This excitatory mechanism is opposite to the inhibitory effects of
30 ethanol at NMDAR. Understanding the active compounds that arise from ethanol metabolism, and
31 the molecular mechanisms by which they influence alcohol reward and cardiovascular function,
32 may be beneficial in developing targeted intervention strategies for both alcohol use disorder and
33 its cardiovascular sequelae.

34

35

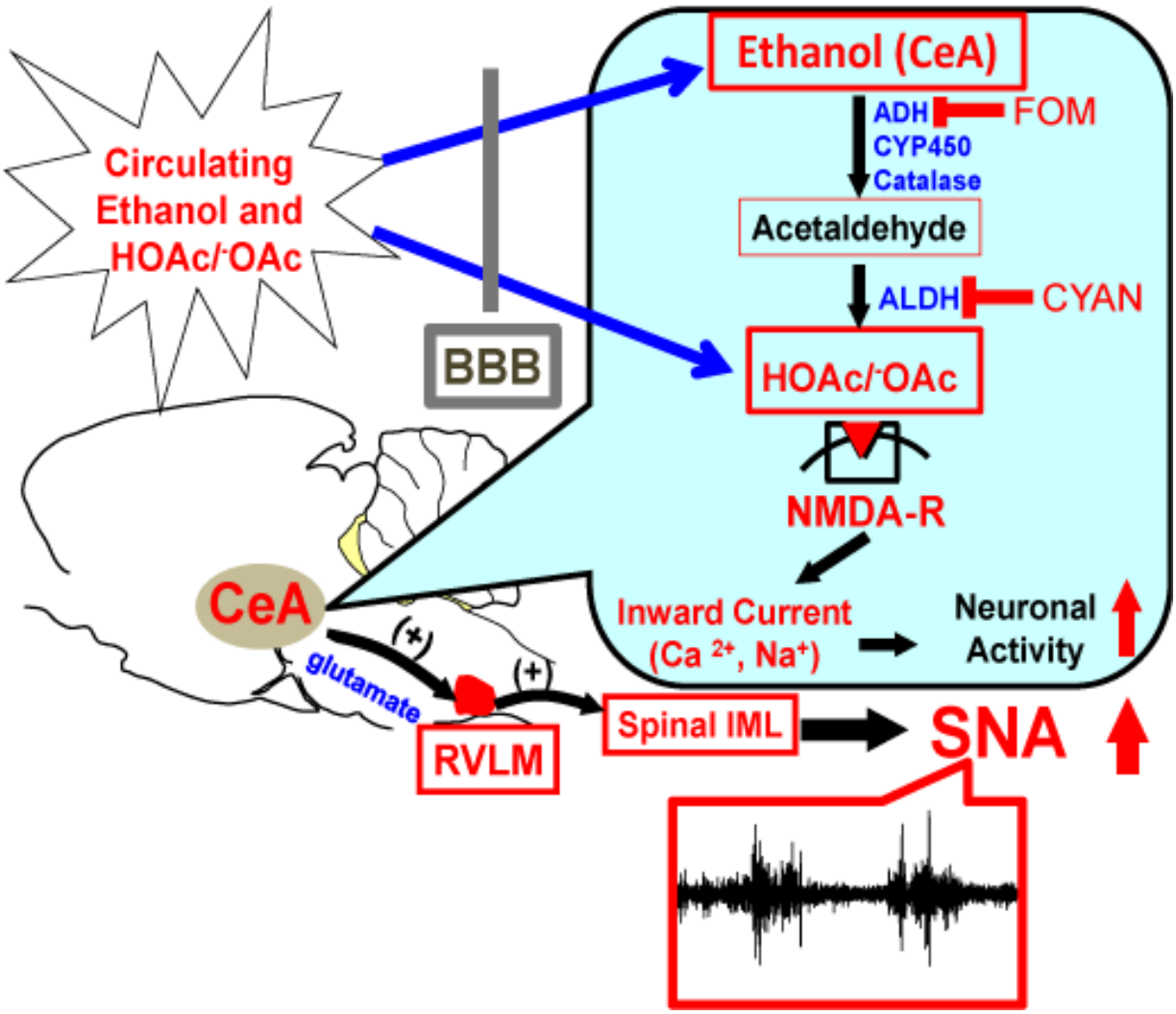

Graphical Figure. Proposed mechanisms for ethanol and acetate induced increases in sympathoexcitation within the central nucleus of the amygdala (CeA). Abbreviations: Acetic acid (HOAc), acetate (⁻OAc), ADH (alcohol dehydrogenase), ALDH (aldehyde dehydrogenase), BBB (blood brain barrier), FOM (fomepizole), CYAN (cyanamide), CYP450 (cytochrome P450), IML (intermediolateral nucleus), RVLM (rostral ventrolateral medulla), SNA (sympathetic nerve activity).

INTRODUCTION

Alcohol is one of the most widely used and abused recreational substances globally. Ethanol metabolism generates acetic acid, which is the main component of vinegar and is produced in large quantities following ethanol ingestion. This leads to significantly elevated serum and cerebrospinal fluid (CSF) acetate concentrations of around 1-3 mM (1, 2) and 2-5 mM (1, 2), respectively. Concentrations of acetic acid/acetate in the circulation and CSF are reported to remain elevated long after ethanol has cleared the body (2). It is therefore reasonable to suspect that acetic acid/acetate may be a player in the altered neuronal function following ethanol consumption and metabolism.

Precisely how ethanol produces excitatory effects in the central nervous system (CNS) is largely unknown. On the one hand, increases in dopamine release from the ventral tegmental area (3) facilitate reward and possible excitatory actions on neurons post ethanol ingestion. However, this is partially contradicted by ethanol itself inhibiting NMDAR in slice recordings (4-6). Secondly, studies involving NMDAR inhibition by ethanol are commonly done in brain slice preparation (4, 5, 7) with large circulating volumes of ethanol relative to small tissue samples, and the effects of in-slice metabolism of ethanol has yet to be reported. What is known is that ethanol consumption contributes to excitatory actions originating within the CNS (3, 8) with some positive modulatory action on NMDAR (9). Excitation is augmented following ethanol clearance, which can lead to hangover symptoms (10, 11). Acetate has been implicated in this response (12). Unfortunately, literature investigating the influence of acetic acid/acetate on neuronal function remains scarce.

Our lab has been pursuing a line of thought that acetic acid/acetate is responsible for many of the excitatory effects of ethanol metabolism on neurons. We have previously reported that

69 microinjection of ethanol and acetate into the central nucleus of amygdala (CeA), an area
70 containing autonomic neurons with axons projecting to the rostral ventrolateral medulla (CeA-
71 RVLM), induced sympathoexcitation and pressor responses mediated by local activation of
72 NMDAR (13). Similarly, we have demonstrated that pathophysiological concentrations of acetate
73 from ethanol metabolism are cytotoxic in dopaminergic-like PC12 cells, at least partially through
74 NMDAR activation (14) and acetic acid increases excitability in medium spiny neurons of the
75 nucleus accumbens shell (15). Given these parallel and converging sets of results, we hypothesized
76 that inhibition of ethanol metabolism (Figure. 1A) may attenuate the ethanol sympathoexcitatory
77 response by preventing the generation of acetic acid/acetate which we have found to activate
78 NMDAR. Similarly, we hypothesized that in brain slice recordings containing CeA-RVLM
79 neurons, bath application of acetate would increase neuronal excitability through activation of
80 NMDAR.
81

82 **MATERIALS AND METHODS**

83 **Animals**

84 Male Sprague-Dawley rats purchased from Charles River Labs (Wilmington, MA, USA)
85 were individually housed in a temperature-controlled room (22-23 ^{o} C) with a 12:12 h light-dark
86 cycle. Chow and tap water were available *ad libitum* unless otherwise noted. All experimental and
87 surgical procedures were carried out under the guidelines of the National Institutes of Health Guide
88 for the Care and Use of Laboratory Animals with the approval of the Institutional Animal Care and
89 Use Committee at Michigan Technological University.
90

91 ***In vivo* whole animal recordings of arterial blood pressure (ABP), splanchnic sympathetic**
92 **nerve activity (SSNA) and lumbar sympathetic nerve activity (LSNA)**

93 Animal surgery was performed following the previously described protocol (16). On the
94 day of the experiment, rats were anesthetized with an intraperitoneal injection containing a mixture
95 of α-chloralose (80 mg/kg) and urethane (800 mg/kg). Adequate depth of anesthesia was assessed
96 before surgery by the absence of the pedal withdrawal reflex and corneal reflexes. Animals were
97 instrumented with an arterial catheter inserted into the aorta through a femoral artery. The catheter
98 was connected to a pressure transducer to measure arterial blood pressure. Heart rate (HR) was
99 obtained from the R-wave of the electrocardiogram (ECG) (lead I). A catheter was also placed in
100 the left femoral vein to administer drugs. After tracheal cannulation, rats were paralyzed with
101 gallamine triethiodide (25 mg·kg−1·h−1 iv) and artificially ventilated with oxygen-enriched room
102 air. After paralysis, adequate depth of anesthesia was determined by lack of pressor responses to
103 noxious foot pinch. Supplemental doses of anesthesia equal to 10% of the initial dose were given
104 when needed. End-tidal PCO_2 was continuously monitored and maintained within normal limits
105 (35–40 mmHg) by adjusting ventilation rate (70–80 breaths/min) and/or tidal volume (2.0–3.0 ml).
106 Body temperature was held at 37°C with a water-circulating pad.

107 SSNA and LSNA recordings were performed according to previously described protocols
108 (13, 16, 17). With the use of a left flank incision, a left lumbar and postganglionic splanchnic
109 sympathetic nerve bundle was isolated from surrounding tissue and mounted on a stainless steel
110 wire electrode (0.127-mm OD; A-M Systems), and covered with a silicon-based impression
111 material (Coltene, Light Body) to insulate the recording from body fluids. The recorded signal was
112 directed to an AC amplifier (P511; Grass Technologies) equipped with half-amplitude filters (band
113 pass: 100-1,000 Hz) and a 60-Hz notch filter. The processed signal was rectified, integrated (10-

114 ms time constant), and digitized at a frequency of 5,000 Hz using a 1401 Micro3 analog-to-digital
115 converter and Spike 2 software (7.04 version; Cambridge Electronic Design, Cambridge, UK).
116 The background noise was determined by a bolus injection of hexamethonium (30 mg/kg iv), a
117 ganglionic blocker, at the end of the experiment and was subtracted from all the integrated values
118 of sympathetic nerve activity.
119

120 **CeA microinjection**

121 CeA injections were performed as previously described (13). Animals were placed in a
122 stereotaxic head frame, and the skull was leveled between bregma and lambda. A section of skull
123 was removed so that a single-barreled glass microinjector pipette could be lowered vertically into
124 the CeA. The following stereotaxic coordinates were used: CeA, caudal to bregma, −2.4 ~ −2.5
125 mm; lateral to midline, 4.8~5.0 mm; and ventral to dura, 7.7~8.0 mm. All animals were allowed
126 to stabilize at least 2 h following surgery. To test whether inhibition of ADH and ALDH prevented
127 ethanol elicited sympathoexcitatory responses, ethanol (1.7 μmol) or a cocktail of ethanol (1.7
128 μmol) and fomepizole (10 nmol) or ethanol (1.7 μmol) and cyanamide (0.24 nmol) were
129 microinjected into the CeA in separate groups of animals. Similarly, the effects of acetate and the
130 involvement of NMDAR on acetate evoked sympathoexcitatory response were also explored
131 through CeA injection of acetate (0.1 μmol and 0.20 μmol) and a cocktail containing acetate (0.20
132 μmol) and memantine (3.0 nmol), or acetate (0.2 μmol) and AP5 (3.0 nmol) (13, 18) in separate
133 groups of animals. Likewise, to verify lack of involvement of cyanamide in the acetate response,
134 a cocktail of acetate (0.20 μmol) and cyanamide (0.24 nmol) was microinjected in separate groups
135 of animals. All compounds were microinjected in a volume of 100 nL with a pneumatic pump
136 (WPI). The volume of each injection was determined by measuring the movement of the fluid

137 meniscus within the microinjector pipette using a dissecting microscope equipped with an eyepiece
138 reticule. At the end of each experiment, Chicago blue dye solution (2% in saline, 100 nL) was
139 injected into the CeA to mark the site of each injection. Brains were removed and post fixed for 5
140 days at room temperature in 4% paraformaldehyde. Brain coronal sections containing the CeA
141 were cut, and microinjection sites were identified under light microscopy. Rats with injection
142 site(s) not inside the CeA were excluded from data analysis.
143

144 **Retrograde labeling**

145 Retrograde labeling of CeA-RVLM neurons(13): Male Sprague-Dawely rats (350-450 g)
146 were retrograde labeled from the RVLM to the CeA. Rats were anesthetized with an intraperitoneal
147 injection (i.p.) of sodium pentobarbital (50 mg/kg), placed in a stereotaxic frame, leveled between
148 bregma and lambda and the skull exposed with a midline incision. A small, unilateral burr hole
149 was drilled to expose the cerebellum in the caudal section of the skull and a glass micropipette
150 lowered into the pressor region of the RVLM (coordinates: −12.7 mm caudal to bregma, 1.8 mm
151 lateral to midline and 8.9 mm below the skull) (19). 100 nL fluospheres (Life Technologies) was
152 injected into the RVLM using a pneumatic pump (WPI) and left in place for approximately 5
153 minutes to prevent tracer backflow. The midline incision was closed, and the rats were
154 administered a subcutaneous (s.c.) injection of penicillin G (30,000 units) and Metacam (1 mg/kg,
155 NSAID) in 0.5 mL saline for three days post-surgery to prevent infection and reduce pain.
156

157 **Whole-cell patch clamp recordings**

158 Five to seven days post labeling, rats were anesthetized with isoflurane (3% in O_2) and
159 decapitated. The brain was rapidly removed and chilled in ice cold cutting solution, containing (in

160 mM): 206 sucrose, 2 KCl, 2 $MgSO_4$, 1.25 NaH_2PO_4, 26 $NaHCO_3$, 1 $CaCl_2$, 1 $MgCl_2$, 10 d-glucose,
161 and 0.4 ascorbic acid, osmolarity 295-302 mosmol L^{-1} measured with an osmometer (Wescor), pH
162 7.3-7.4, continuously gassed with 95:5 O_2:CO_2 to maintain pH and pO_2. A brain block was cut
163 including the CeA region and affixed to a vibrating microtome (Leica VT 1000S; Leica, Nussloch,
164 Germany). Coronal sections of 250 µm thickness were cut, and the slices transferred to a holding
165 container of artificial cerebral spinal fluid (ACSF) maintained at 30 °C, continuously gassed with
166 95:5 O_2:CO_2, containing (in mM): 125 NaCl, 2 KCl, 2 $MgSO_4$, 1.25 NaH_2PO_4, 26 $NaHCO_3$, 2
167 $CaCl_2$, 10 d-glucose, and 0.4 ascorbic acid (osmolality: 295–302 mosmol L^{-1}; pH 7.3-7.4) and
168 allowed to recover for 1 hr. Following recovery, slices were transferred to a glass-bottomed
169 recording chamber and viewed through an upright microscope (E600FN, Nikon) equipped with
170 DIC optics, epi-fluorescence, an infrared (IR) filter and an IR-sensitive video camera (C2400,
171 Hamamatsu, Bridgewater, NJ).

172 Slices transferred to the glass-bottomed recording chamber were continuously perfused
173 with ACSF, gassed with 95:5 O_2:CO_2, maintained at 30 °C and circulated at a flow of 2 mL min^{-}
174 ^{1}. Patch electrodes were pulled (Flaming/Brown P-97, Sutter Instrument, Novato, CA) from
175 borosilicate glass capillaries and polished to a tip resistance of 4–8 MΩ. Electrodes were filled
176 with a solution containing (in mM) 135 K-gluconate, 10 HEPES, 0.1 EGTA, 1.0 $MgCl_2$, 1.0 NaCl,
177 2.0 Na_2ATP, and 0.5 Na_2GTP (osmolality: 280–285 mosmol L^{-1}; pH 7.3). Once a GΩ seal was
178 obtained, slight suction was applied to break into whole-cell configuration. The cell was allowed
179 to stabilize; this was determined by monitoring capacitance, membrane resistance, access
180 resistance and resting membrane potential (V_m) (19). Records were not corrected for a liquid
181 junction potential of -15 mV. Cells that met the following criteria were included in the analysis:
182 action potential amplitude ≥50 mV from threshold to peak, input resistance (R_{input}) >0.3 GΩ

183 (determined by injection of −20 pA from a holding potential of −80 mV), resting V_m negative to
184 −50 mV, and <20% change in series resistance during the recording. Recordings were made using
185 an Axopatch 200B amplifier and pCLAMP software (v10.2, Axon Instruments, Union City, CA).
186 Signals were filtered at 1 kHz, digitized at 10 kHz (Digidata 1400A, Axon Instruments), and saved
187 on a computer for off-line analysis. To study the mAHP as we have previously reported,(19)
188 recordings were made from a potential of −60 mV, and +150 pA current injection (500 ms) were
189 made followed by a return of V_m to −60 mV for 5 s.

190 The effect of acetate on the excitability of CeA-RVLM neurons and the role of NMDAR
191 (current-clamp): With V_m adjusted to -80 mV by continuous negative current injection, a series of
192 square-wave current injections was delivered in steps of +25 pA, each for a duration of 800 ms.
193 To determine the action potential voltage threshold (Vt or rheobase) and depolarizing R_{input} below
194 V_t, ramp current injections (0.2 pA/ms, 1,000 ms) were made from a potential of -80 mV. Square-
195 wave and ramp current injections were made in the same neurons. Effects of acetate on neuronal
196 excitability were determined by comparing current evoked spike frequency responses under
197 control conditions with responses recorded from neurons exposed to bath application of acetate.
198 To determine the dose-dependent response, the effect of various concentration of acetate (0.0, 3.75,
199 7.5, 37.5 and 75.0 mM) on the excitability was determined in separate groups of neurons,
200 respectively. To test whether the activation of NMDAR was involved in the increased neuronal
201 excitability elicited by acetate, the effect of bath application of AP5 (60 μM, NMDAR competitive
202 blocker) or memantine (30 μM, NMDAR pore blocker), on the excitability was determined in the
203 presence of acetate (37.5 mM) in a separate group of neurons. To determine the slope of the current
204 injection response (another measure of how excitable neurons are over a range of current
205 injection), a linear regression was fit to each treatment group (control, NaOAc, NaOAc & AP5 and

206 NaOAc & memantine), between 0 and 250 pA. The slope of each current injection response (gain)
207 ± SEM were compared across groups.

208 Acetate evoked inward current and the role of NMDAR (voltage-clamp) in CeA-RVLM
209 neurons: Brain slices were continuously perfused with modified, Mg^{2+} free ACSF containing (in
210 mM): 127 NaCl, 2 KCl, 1.25 NaH_2PO_4, 26 $NaHCO_3$, 2 $CaCl_2$, 10 d-glucose, and 0.4 ascorbic acid
211 (osmolality: 295–302 mosmol L^{-1}; pH 7.3-7.4), gassed with 95:5 O_2:CO_2, maintained at 30 °C and
212 circulated at a flow of 2 mL min^{-1}. Tetrodotoxin (TTX, voltage gated sodium channel blocker, 0.5
213 μM) and picrotoxin (GABA-A blocker, 100 μM) were added into the circulating extracellular,
214 Mg^{2+} free ACSF. Cells were voltage clamped at V_m = -80 mV and allowed to stabilize by
215 monitoring baseline current. Once cells were stable and baseline recording in the absence of acetate
216 ~1.5 min was observed, acetate (37.5 mM) was added to the circulating bath and recorded until a
217 plateau was observed > 15 min. At this point, washout and recovery was observed. To test whether
218 the activation of NMDAR was involved in the inward current evoked by acetate, the effect of
219 memantine (30 μM) or AP5 (60 μM) on the inward current was determined. In separate groups of
220 neurons, acetate (37.5 mM) and memantine (30 μM) or acetate (37.5 mM) and AP5 (60μM) were
221 added to the circulating bath and the inward current was observed. To exclude the possibility that
222 the inward current evoked by sodium acetate was due to the increase in extracellular sodium
223 concentration, equimolar sodium gluconate (37.5 mM) was substituted for sodium acetate and the
224 inward current was recorded.

225 Note that current- and voltage-clamp recordings were made from separated groups of CeA-
226 RVLM neurons. Passive membrane properties (capacitance, resting membrane potential and
227 hyperpolarizing input resistance) to each drug treatment protocol are reported in table 1.
228

229 **Preparation of neuronal cultures**

230 Whole brain neuronal cultures were made from 1-day old SD rats according to our previous
231 publication.(20, 21) Briefly, rats were anesthetized with pentobarbital (50 mg/kg) and the brains
232 were extracted and dissected. Dissected brain areas were combined, and brain cells were
233 dissociated before being plated on poly-L-lysine precoated culture dishes. Two days following
234 plating, cultures were treated for two days with cytosine arabanoside (ARC, 10 μM) to kill off
235 rapidly dividing cells (astroglia and astrocytes) followed by fresh ARC free media for the
236 remainder of cultures. Neuronal cultures contained > 90% neurons with the remainder primarily
237 astroglia. Neuronal cell cultures were grown for 10-14 days before use in cell culture experiments.
238

239 **Real-time calcium imaging**

240 Primary neuronal cultures 12-14 days post isolation were incubated for 30 min with Fluo-
241 4AM (Thermofisher, 3 μM final concentration) according to the manufactures instructions in
242 artificial cerebral spinal fluid (ACSF), containing (in mM): 125 NaCl, 2 KCl, 2 $MgSO_4$, 1.25
243 NaH_2PO_4, 26 $NaHCO_3$, 2 $CaCl_2$, 10 d-glucose, and 0.4 ascorbic acid (osmolality: 295–302 mosmol
244 L^{-1}; pH 7.3-7.4) in a 5% CO_2 humidified incubator at 37 °C. The staining solution was aspirated
245 and fresh ACSF (0.5 mL) added to the cells. Baseline calcium fluorescence were taken followed
246 by the addition of acetate and/or acetate and memantine in ACSF (0.5 mL additional volume
247 added) to reach the desired concentrations (e.g., 0.5 mL ACSF initial, then add 0.5 mL acetate (75
248 mM) in ACSF. Final concentration acetate (37.5 mM)). Images were captured for each well in a
249 24 well plate using a cell imager equipped with the correct LED lights (ZOE, Bio-Rad).
250 Fluorescence intensity was analyzed and quantified using ImageJ software(22) on 10-13 randomly
251 selected cells for each treatment and corrected fluorescence intensity (CFIT) compared between

252 treatment groups prior to adjusting backgrounds. CFIT was calculated based on individual
253 background fluorescence within each well, prior to batch background normalization for image
254 preparation. Duplicates of each treatment were compared, and all showed similar trends. Negative
255 controls were run for ACSF alone on time course for alterations in baseline calcium and there was
256 no significant change in baseline values compared to 25 minutes post ACSF only.
257
258 **Justification on doses/concentrations**
259 To verify the effects of ethanol in the CeA, we selected a dose of ethanol (1.7 µmole or
260 100 nL of 17.15 M) which was a dose we found to yield a maximum response *in vivo* as previously
261 described.(13) Previous studies of targeted brain delivery of ethanol to the CeA in rats (75-350
262 mg%, consisting of 8,000-10,000 nL infusions or a total dose of 0.761 µmole ethanol) (23) have
263 been reported, and our maximum dose utilized is close to this dosing regimen. The following
264 acetate doses were used for *in vivo* CeA microinjections: 0.1 and 0.2 µmole or 100 nL of 1 M and
265 2 M sodium acetate. Previous intraventricular infusions (0.8-2.8 µmole) of acetate have been
266 reported (24) and we are within acceptable limits.
267 For our electrophysiology experiments, we utilized the current ethanol metabolism profile
268 (roughly 90% of ethanol is metabolized to acetic acid/acetate) (25). That is to say, ethanol
269 metabolism to acetic acid/acetate is a 1:1 conversion and apparent ethanol concentrations
270 measured would in theory produce equivalent acetic acid/acetate concentrations (e.g., 50 mM
271 ethanol should equal 50 mM acetate). We constructed a dose-dependent response curve to acetate
272 and found an EC_{50} of 5.90 mM and an E_{max} of 37.5 mM. We utilized 37.5 mM for our
273 electrophysiology studies because it yielded the most robust response.
274

275 **Computational modeling**

276 The NR1/NR2A NMDAR (2A5T) crystal structure (26) was downloaded from the protein
277 databank (PDB). Acetic acid, glutamic acid, glutaric acid, glycine and AP5 structures were
278 downloaded from PubChem. All structures were imported into PyRx (27) and a docking box
279 measuring (4.3x7.3x5.0 angstrom) was made around native glutamate. In a separate set of
280 experiments, a docking box measuring (3.5x4.9x4.1 angstrom) was made around native glycine.
281 Prior to computational docking, native glutamate or glycine was removed and each structure was
282 docked for 8 iterations. Docking outputs were imported in PyMol(28) for display and
283 ligand/receptor interaction purposes.

284

285 **Chemicals**

286 All chemicals were obtained from Sigma-Aldrich (St Louis, MO, USA) with the exception
287 of tetrodotoxin (Tocris Bioscience, UK) and tetraethylammonium sodium (Fluka BioChemika,
288 Switzerland). Glacial acetic acid was obtained from Sigma-Aldrich (St. Louis, MO) and ultra-pure
289 water (> 18 MΩ) obtained in-house by filtration and purification of house distilled water from an
290 EasyPure II water filtration system (Barnstead).

291

292 **Statistical analysis**

293 Data values were reported as mean ± SEM. Depending on the experiments, group means
294 were compared using either paired, unpaired Student's *t*-test, a one-way or a two-way ANOVA.
295 Differences between means were considered significant at $p < 0.05$. Where differences were
296 found, Bonferroni post hoc tests were used for multiple pair-wise comparisons. All statistical

297 analyses were performed with a commercially available statistical package (GraphPad Prism,
298 version 9.0).
299
300 **RESULTS**
301 **Local metabolism of ethanol to acetic acid/acetate in the CeA activates NMDAR *in vivo***
302 Our lab previously reported that ethanol and acetate microinjected into the CeA of
303 anesthetized rats resulted in a sympathoexcitatory effect and speculated that it was due to local
304 metabolism of ethanol to acetate (13). Consistent with our previous findings, microinjection of
305 ethanol into the CeA of anesthetized rats elicited a sympathoexcitatory and pressor response
306 (Figure 1B,E,F). Because we speculated that this sympathoexcitatory response was due to local
307 metabolism of ethanol to acetate, we co-applied ethanol with an alcohol dehydrogenase inhibitor
308 (ADH), fomepizole (29) or an aldehyde dehydrogenase inhibitor (ALDH), cyanamide (30), into
309 the CeA (Figure 1C,D). Blockade of ADH with fomepizole or ALDH with cyanamide significantly
310 blunted the sympathoexcitatory response from ethanol (one-way ANOVA, $p<0.0001$, Figure 1),
311 indicating that neither ethanol nor acetaldehyde was likely a causitive agent in the excitatory
312 response. Summary data for change in SSNA and MAP in response to ethanol, ethanol +
313 fomepizole or ethanol + cyanamide are displayed in Figure 1. Cyanamide (0.24 nmole) alone had
314 no significant effect on SSNA (pre: 0.04 ± 0.009 vs post: 0.04 ± 0.008, $p=0.3016$, paired t-test),
315 LSNA (pre: 0.015 ± 0.004 vs post: 0.020 ± 0.005, $p=0.10$, paired t-test) or MAP (pre: 113 ± 6.0
316 vs post: 104 ± 8.0, $p=0.0734$, paired t-test) (n=5 rats).
317 Next, we verified that acetate was the bioactive metabolite from ethanol metabolism.
318 Microinjection of acetate into the CeA of anesthetized rats increased sympathetic nerve activity
319 and mean arterial blood pressure (MAP) in a dose-dependent manner (Figure 2). For NMDAR

320 antagonism, memantine has seen utilization in alcohol studies (31, 32) to prevent cognitive decline
321 and as a possible therapeutic for excitotoxicity (33). Furthermore, it is an FDA approved NMDAR
322 blocker for the treatment of Alzhiemer's disease (34), and has been shown to prevent alcohol
323 craving in humans (35). The use of memantine would be anticipated to give more powerful
324 treatment options clinically compared to utilizing AP5 as previously described (13) or MK-801
325 (Olney's lesions) (36). Blockade of NMDAR within the CeA using memantine or AP5
326 significantly attenuated the acetate induced sympathoexcitatory and pressor responses (one-way
327 ANOVA, $p<0.05$, Figure 2A,B,C) suggesting that increases in SNA were due to acetate activation
328 of NMDAR (Figure 2). Memantine (3.0 nmole) alone had no significant effect on baseline MAP
329 (pre: 112 ± 7.63 vs post: 110.3 ± 8.67, $p=0.58$, paired t-test), SSNA (pre: 0.023 ± 0.008 vs post:
330 0.024 ± 0.009, $p=0.37$, paired t-test) and LSNA (pre: 0.018 ± 0.002 vs post: 0.019 ± 0.002, $p=0.14$,
331 paired t-test) (n=3 rats). Likewise, our previous study utizling AP5 saw no significant difference
332 to CeA microinjected AP5 on baseline parmeters (13).

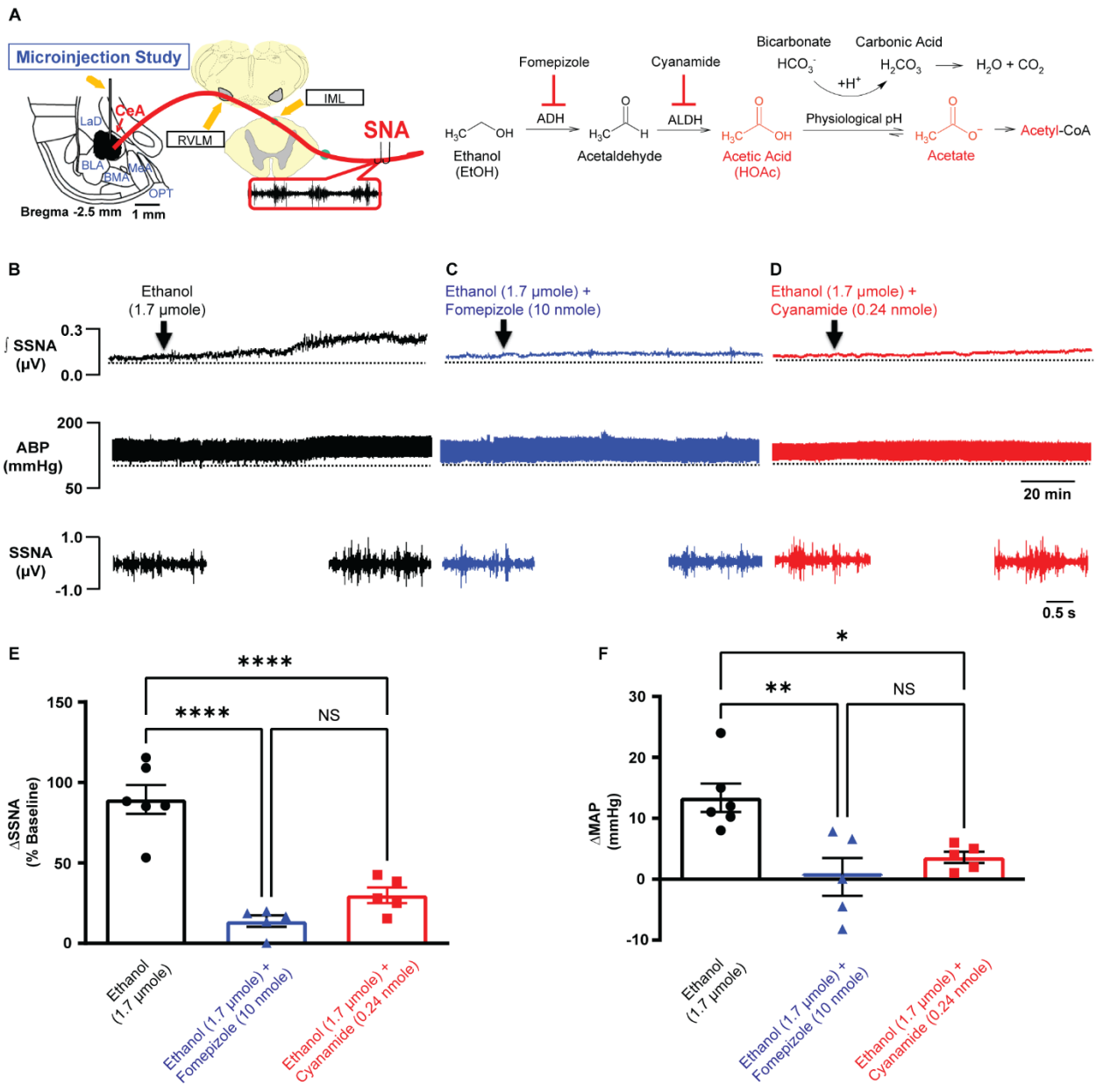

Figure 1. Local CeA brain metabolism of ethanol is sympathoexcitatory. (A) Graphical depection of CeA microinjection study for sympathetic nerve recordings (left). Metabolic pathway of alcohol metabolism (right). **(B)** Representative raw traces displaying SSNA and arterial blood pressure (ABP) from CeA microinjected ethanol. **(C)** Representative raw traces displaying SSNA and arterial blood pressure (ABP) from CeA microinjected ethanol + fomepizole. **(D)** Representative raw traces displaying SSNA and arterial blood pressure (ABP) from CeA

340 microinjected ethanol + cyanamide. **(E)** Summary data of SSNA for ethanol (black), ethanol +
341 fomepizole (blue) and ethanol + cyanamide (red) (****$p<0.0001$). **(F)** Summary data of change
342 in mean aterial pressure (MAP) for ethanol (black), ethanol + fomepizole (blue) and ethanol &
343 cyanamide (red), (n=number of rats) (**$p=0.0043$, *$p=0.029$). Abbreviations: ADH, alcohol
344 dehydrogenase; ALDH, aldehyde dehydrogenase).

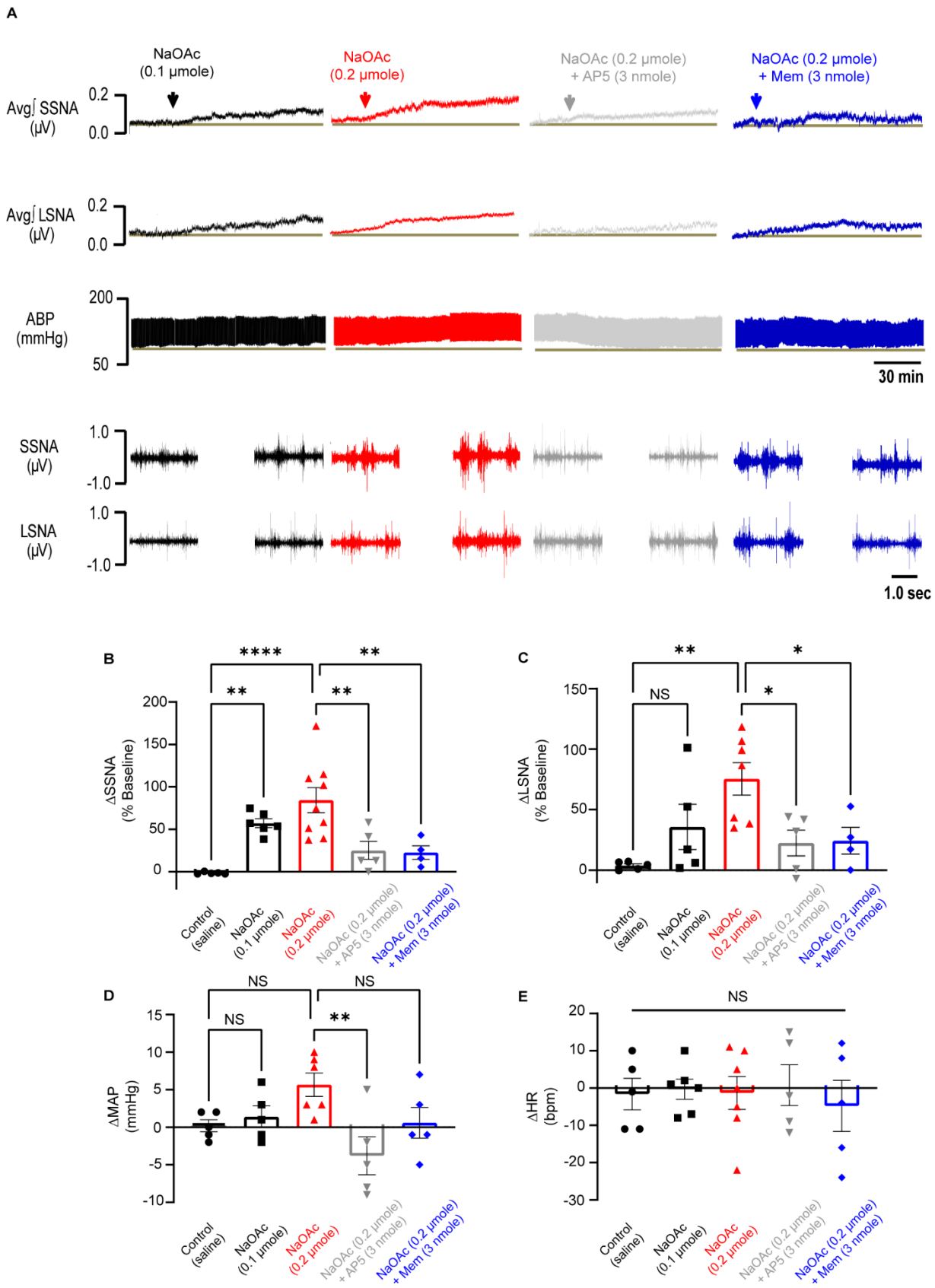
A
NaOAc (0.1 µmole)
NaOAc (0.2 µmole)
NaOAc (0.2 µmole) + AP5 (3 nmole)
NaOAc (0.2 µmole) + Mem (3 nmole)
Avg∫ SSNA (µV)
Avg∫ LSNA (µV)
ABP (mmHg)
30 min
SSNA (µV)
LSNA (µV)
1.0 sec
B
ΔSSNA (% Baseline)
C
ΔLSNA (% Baseline)
D
ΔMAP (mmHg)
E
ΔHR (bpm)
Control (saline)
NaOAc (0.1 µmole)
NaOAc (0.2 µmole)
NaOAc (0.2 µmole) + AP5 (3 nmole)
NaOAc (0.2 µmole) + Mem (3 nmole)
NS

345

346 **Figure 2. CeA microinjected acetate dose-dependently increases sympatheic nerve activity**
347 **and is NMDAR dependent. (A)** Representative raw traces displaying sympathetic nerve activity
348 (SSNA and LSNA) and ABP from CeA microinjected acetate. **(B)** Summary SSNA data
349 (**p=0.0093, **** p<0.0001). **(C)** Summary LSNA data (*p=0.045, **p=0.018). **(D)** Summary
350 MAP data (**p=0.003). **(E)** Summary change in HR data (NS=not significant), (individual
351 points=number of animals).
352

353 **Estimating final CeA tissue concentrations from microinjection**

354 Estimation of brain microinjected compounds is a notoriously difficult task. Small
355 volumes, effects of anesthesia, and blood flow drastically alter what local brain area tissues are
356 exposed to in terms of final concentrations. The ethanol literature reports ~90% ethanol
357 metabolism to acetic acid/acetate, and this conversion is 1:1 (25). Reported intoxicating blood
358 alcohol concentrations in humans and rodents typically fall in the range of 17-100 mM (37-39),
359 with measurements in the cerebellum of around 90 mM (40). However, brain slice patch clamp
360 recordings sometimes utilize ethanol concentrations in excess of 200 mM (41-43). To estimate
361 brain tissue concentrations to compounds tested, we microinjected 100 nL of ethanol or saline
362 loaded with Chicago blue dye within the CeA, collected the stained tissue and recorded the weight.
363 CeA estimated concentrations were determined by [x µmole compound/average tissue volume
364 (mL)]. These concentrations represent the upper theoretical concentration limit and are likely an
365 overestimate as diffusion is greater than the visualized stained tissue excised. Nevertheless, the
366 upper theoretical concentration for 1.7 µmole ethanol is 283 mM, for 0.1 µmole acetate is 16.6
367 mM and for 0.2 µmole acetate is 33.3 mM (Figure 3).

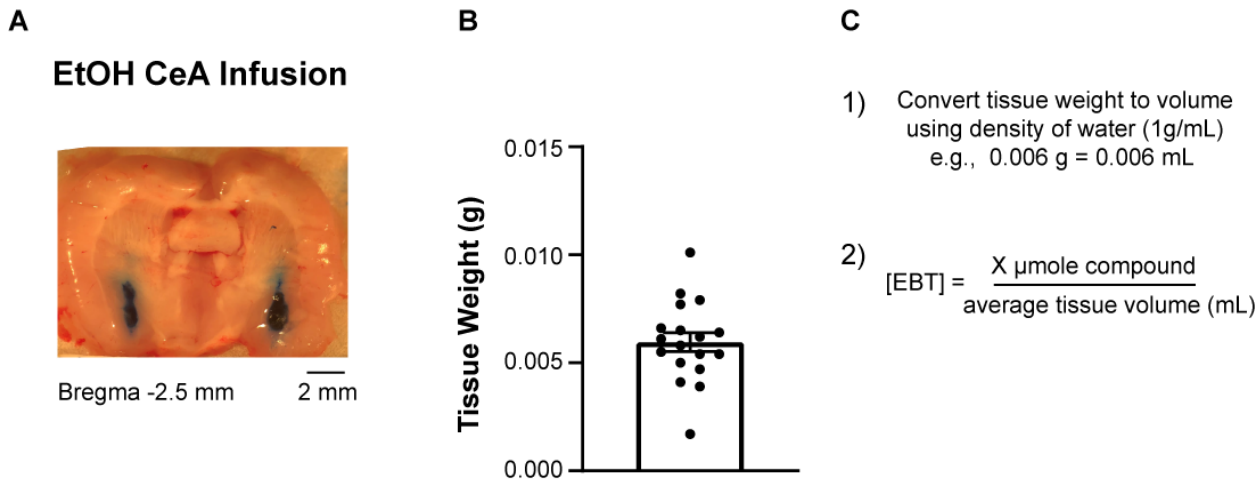

Figure 3. CeA brain tissue concentrations. (A) Representative image of CeA microinjection of 100 nL ethanol loaded with chicago blue dye. **(B)** Excised CeA tissue weights of microinjected ethanol or saline. **(C)** Method for estimating upper theoretical limit of brain tissue concentrations (n=18 CeA tissue samples from N=9 rats). Abbreviations: Estimated brain tissue = EBT.

Bath application of acetate increases CeA-RVLM neuronal excitability through activatation of NMDAR and is not driven by excess extracellular sodium

Our previous *in vivo* microinjection study demonstrated ethanol and acetate induced sympathoexcitation by activation of NMDAR in the CeA through a projection to the rostral ventraolateral medulla (CeA-RVLM) (13). We therefore examined whether acetate was capable of increasing neuronal excitability of CeA-RVLM neurons in brain slice preparation. The RVLM as we and others have previously reported (13, 44, 45) is a key source of sympathoexcitatory drive that can contribute to elevated sympathetic outflow and heavily regulates cardiovascular function. What we found was that extracellular acetate consistently increased CeA-RVLM neuronal excitability in a dose-dependent manner (0.0 mM: 19 ± 1.2 Hz, n=7; 3.75 mM: 21.8 ± 1.6 Hz, n=5, 7.5mM: 36 ± 7.1 Hz, n=6; 37.5 mM: 41 ± 4.1, n=8; 75 mM: 44 ± 5.0, n=7), with an EC_{50} value of

385 5.90 mM (Figure 4) and an E_{max} of 37.5 mM. The EC_{50} value is close to peak acetate concentrations
386 of ~4.60 mM measured by Wang and colleagues in ethanol and acetate infused rats (1) and is also
387 similar to cytotoxic doses we observed in dopaminergic-like PC12 cells (14). Our E_{max} value of
388 37.5 mM was utilized to elicit maximum responses to both intrinsic excitability as well as NMDAR
389 mediated inward currents. A one-way ANOVA with Bonferroni post-hoc test revealed differences
390 ($F_{(4,28)}$ = 6.41, p=0.0009) in firing frequency observed between control vs 7.5 mM, 37.5 mM
391 acetate and control vs 75 mM acetate.

392 To exclude the possibility that increased excitability was driven by excess extracellular
393 sodium concentrations and to verify that NMDAR were involved in the acetate induced increase
394 in CeA-RVLM neuronal excitability, we used sodium gluconate (37.5 mM) as a sodium control
395 and two NMDAR blockers, AP5 and memantine. Sodium gluconate (37.5 mM, N=2 rats, n=3
396 neurons) failed to increase neuronal excitability across the stimulus resopnse curve compared to
397 control cells (two-way ANOVA, p>0.9999). Further analysis at 250 pA current injection also
398 revealed no significant difference between control and sodium gluconate (19.00 ± 1.2 vs 15.00 ±
399 3.75 Hz, unpaired t-test, p=0.2225). Co-application of acetate and AP5 was only able to slightly
400 reduce neuronal excitability (Figure 5A-C) while co-application of acetate and memantine (Figure
401 5A-C) was able to completely abolish the acetate induced increase in CeA-RVLM neuronal
402 excitability. A two-way ANOVA with Bonferroni post-hoc correction of the current stimulus
403 response (Figure 5B) showed significant differences among treatments ($F_{(1,14)}$ = 10.46, p= 0.0060).
404 To understand the net effects of acetate on intrinsic excitability and the involvement of NMDAR
405 over the range of the stimulus response, we analyzed the slope (gain) of each group's curve (0-250
406 pA) using a linear regression. Linear regressions were well fit with R-squared values of (0.96,
407 0.95, 0.90, 0.95 and 0.94) for control, NaOAc, NaOAc & memantine and NaOAc & AP5, and

408 sodium gluconate (37.5 mM) respectively. Acetate significantly increased the slope of the current
409 injection response curve compared to control (0.157 ± 0.007 vs 0.066 ± 0.004 Hz/pA). Acetate
410 and AP5 or acetate and memantine reduced the slopes to 0.1217 ± 0.005 Hz/pA and 0.0761 ± 0.008
411 Hz/pA respectively (Figure 5C). There was no statistical difference between control cells and
412 sodium gluconate (0.066 ± 0.004 Hz/pA vs 0.06619 ± 0.008 Hz/pA, p>0.9999). A one-way
413 ANOVA with Bonferroni post-hoc test revealed differences ($F_{(3,24)} = 47.81$, $p < 0.0001$) between
414 control vs acetate, acetate vs acetate + AP5, and acetate vs acetate + memantine. There was no
415 statistical difference in passive neuronal properties highlighted in Table 1.

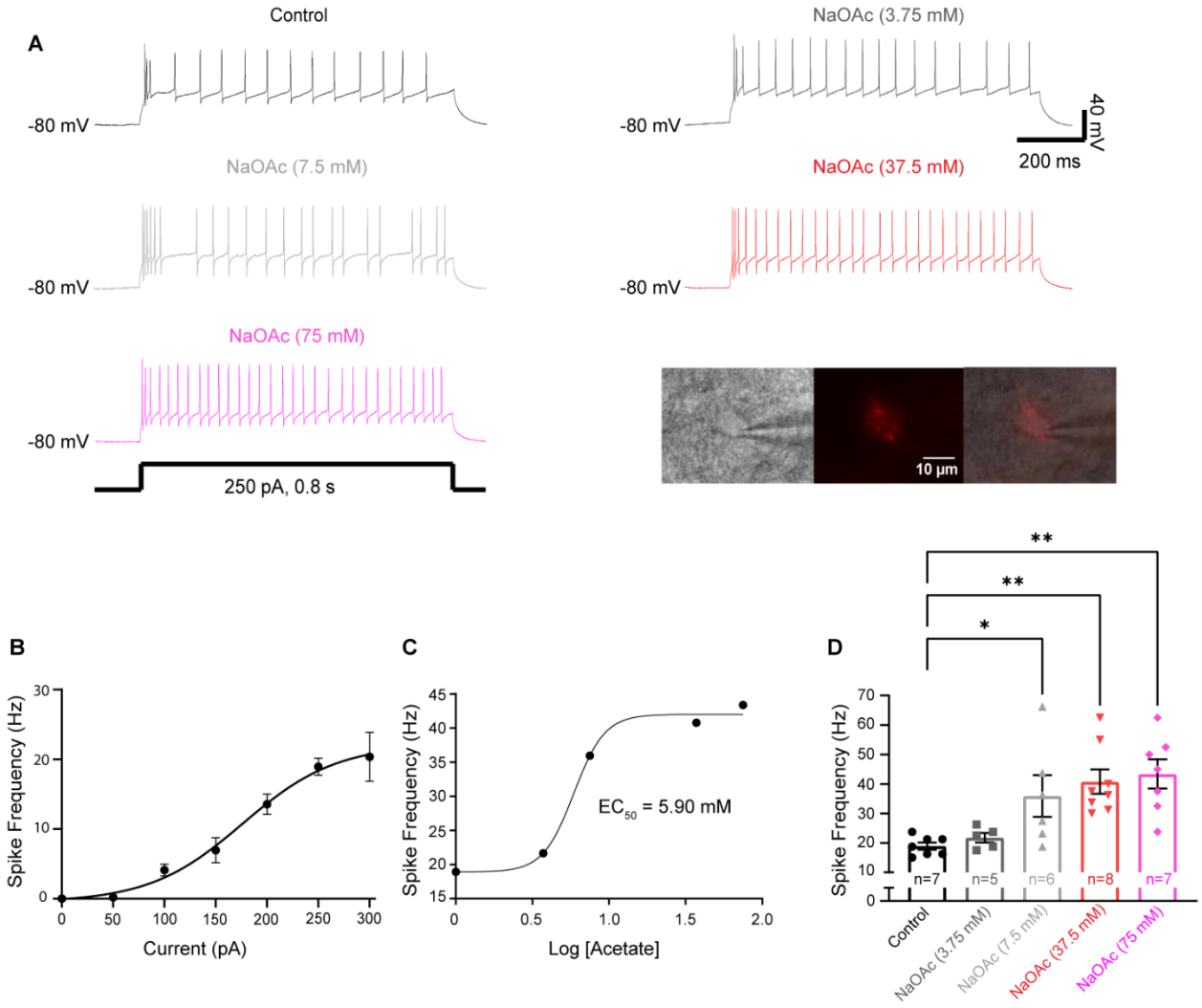

416

417 **Figure 4. Acetate increases CeA-RVLM neuronal excitability in a dose-dependent manner.**
418 **(A)** Representative raw excitability traces for varying doses of acetate to +250 pA current injection
419 and representative CeA-RVLM neuron; differential interference contrast (DIC, left),
420 epifluorescence of the same neuron from retrograde RVLM fluorescent labeling (middle), merged
421 DIC/epifluorescence indicating CeA neuron with projection to RVLM (right). Step-current
422 injection protocol below traces. **(B)** Stimulus response curve for CeA-RVLM neurons (n=7
423 neurons, N=5 rats). Maximum firing occurred at +250 pA current injection. **(C)** Dose-dependent
424 response curve for sodium acetate (NaOAc) on firing frequency at +250 pA current injection. The
425 EC_{50} value for NaOAc was 5.90 mM. **(D)** Summary data for spike frequency at +250 pA current
426 injection in control, and NaOAc (0, 3.75, 7.5, 37.5 and 75 mM) treated CeA-RVLM neurons
427 (*p=0.0474, **p=0.0036, ***p=0.0016 vs control): (n=7 neurons, N=5 rats), (n=5 neurons, N=2
428 rats), (n=6 neurons, N=3 rats), (n=8 neurons, N=3 rats), (n=7 neurons, N=3 rats).
429

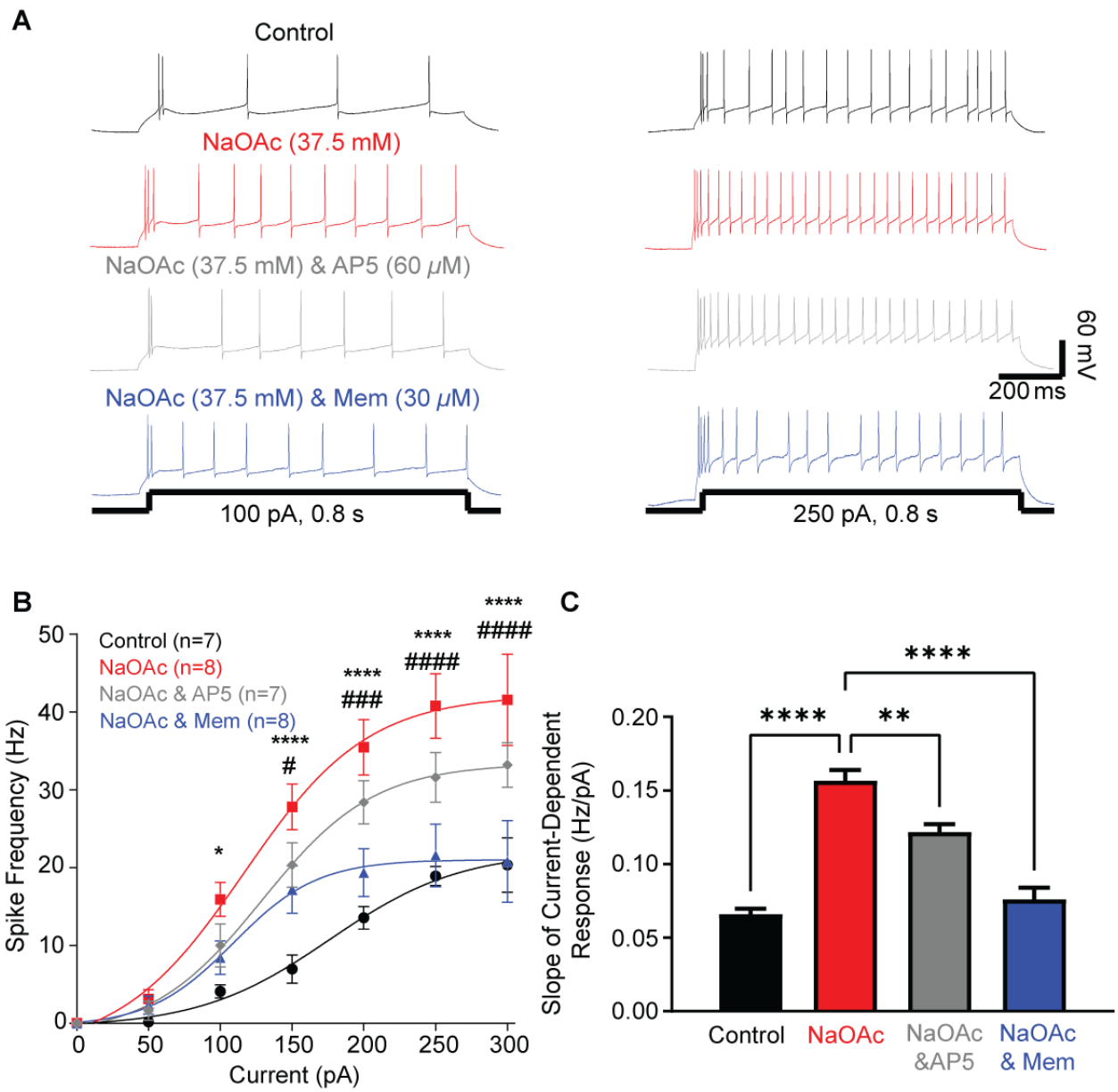

Figure 5. Effect of NMDAR antagonists on acetate induced excitability from current injection step protocol. (A) Representative raw traces for control (black), NaOAc (37.5 mM, red), NaOAc & AP5 (grey) and NaOAc & memantine (blue) at +100 pA (left) and +250 pA (right). Step-current injection protocols below traces. **(B)** Current stimulus response for control (black), NaOAc (red), NaOAc & AP5 (grey) and NaOAc & memantine (blue). (*p<0.05, ****p< 0.0001 NaOAc vs control, # p<0.05, ### p<0.001, ### p<0.0001 NaOAc vs NaOAc & memantine). **(C)** Slope of

437 injected current response for control (black), NaOAc (red), NaOAc & AP5 (grey) and NaOAc &
438 memantine (blue). (****p< 0.0001 vs control, ##p=0.0012, ####p< 0.0001 vs NaOAc) (n=7
439 neurons, N=5 rats), (n=8 neurons, N=3 rats), (n=6 neurons, N=2 rats) (n=6 neurons, N=3 rats).
440

441 **Computational modeling of glutamic acid, acetic acid, glutaric acid, glycine and AP5 with**
442 **NR1/NR2A NMDAR**

443 To help explain the discrepancy between AP5's and memantine's effectiveness in blunting
444 the acetate-induced increase in excitability, we computationally modeled active glutamate site
445 docking and binding affinity with 1) glutamic acid, 2) acetic acid 3) glutaric acid and 4) AP5 in
446 the NR1/NR2A NMDAR(26) (Figure 6). Additionally, we modeled NR1/NR2A glycine site
447 docking and binding affinity with 1) glycine and 2) acetic acid (Figure 6). Modeled structures were
448 overlayed on the native glutamate ligand obtained from x-ray crystallography (2A5T) (26) or
449 native glycine (2A5T). To demonstrate the effectiveness of computational modeling, we first
450 modeled glutamic acid and compared it with natively bound glutamate. We found that
451 computationally modeled glutamic acid orientated similarly to native glutamate (Figure 6) with
452 similar ligand/receptor interactions and a binding affinity of -5.7 kcal/mol. Computationally
453 modeled acetic acid orientated similarly to native glutamate carboxy terminals (Figure 6) with
454 similar ligand/receptor interactions. The 1st binding affinity near the glutamate carboxy location
455 was -3.9 kcal/mol and the 2nd binding affinity for the opposite carboxy terminal was -3.5 kcal/mol.
456 Computationally modeled AP5 also orientated similarly to native glutamate (Figure 6) with similar
457 ligand/receptor interactions and a binding affinity of -5.2 kcal/mol. To model potential binding of
458 two acetic acid molecules simultaneously, glutaric acid was selected as it contains a five-carbon
459 chain with free rotation about the chain's axis and two carboxylic acid terminals (similar to acetic

460 acid and similar to glutamic acid with no amine). Glutaric acid orientated similarly to native
461 glutamate with similar ligand/receptor interactions and a binding affinity of -5.4 kcal/mol.

462 In the glycine binding pocket, computationally docked glycine had similar orientation to
463 native glycine and similar ligand/receptor interactions (Figure 6) with a binding affinity of -3.1
464 kcal/mol. Computationally modeled acetic acid orientated slightly differently that native glycine
465 but had similar ligand/receptor interactions and a calculated binding affinity of -3.1 kcal/mol.

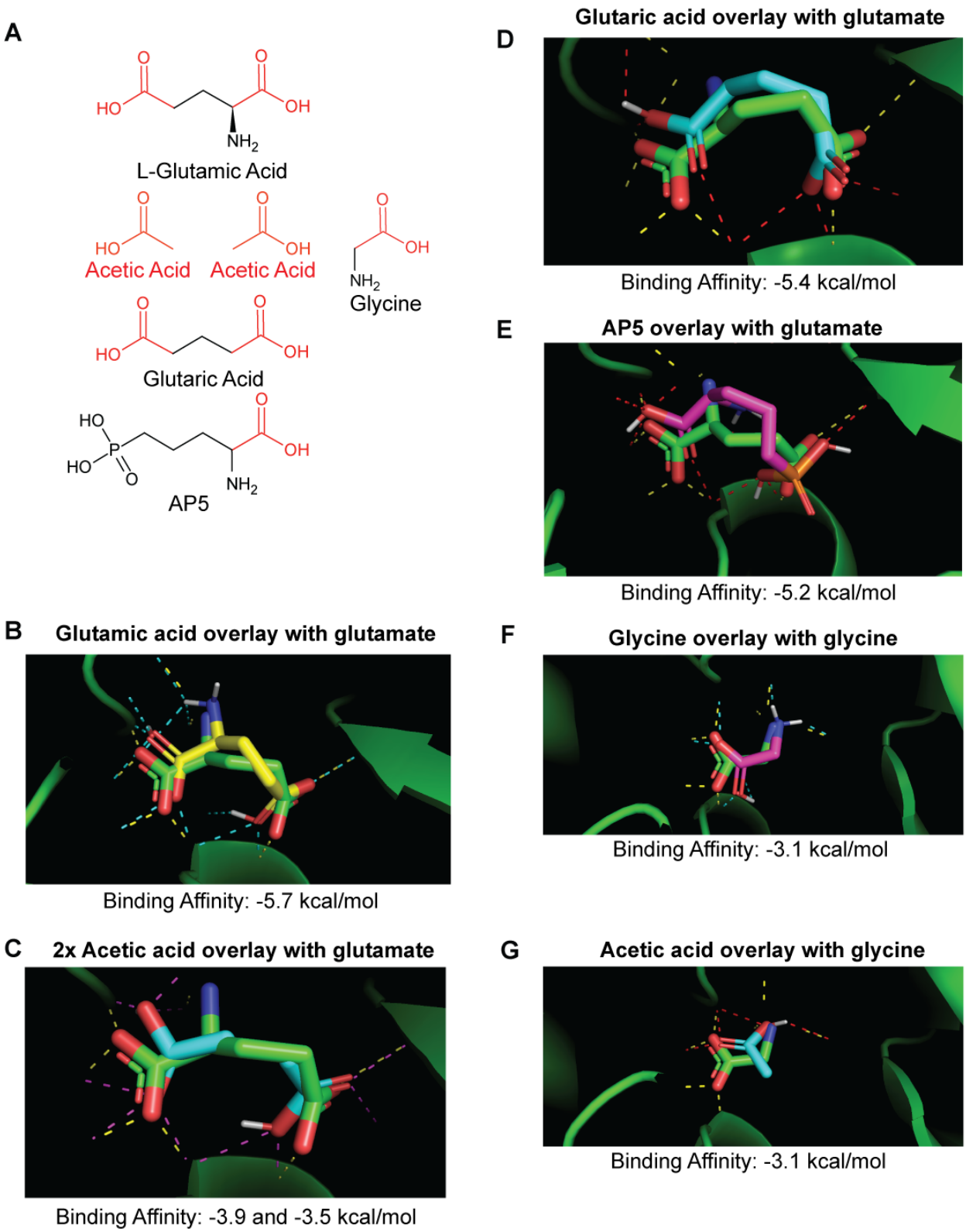
A
HO
O
O
OH
NH2
L-Glutamic Acid
HO
O
Acetic Acid
O
OH
Acetic Acid
O
OH
NH2
Glycine
HO
O
O
OH
Glutaric Acid
HO
HO
P
O
O
OH
NH2
AP5
B
Glutamic acid overlay with glutamate
Binding Affinity: -5.7 kcal/mol
C
2x Acetic acid overlay with glutamate
Binding Affinity: -3.9 and -3.5 kcal/mol
D
Glutaric acid overlay with glutamate
Binding Affinity: -5.4 kcal/mol
E
AP5 overlay with glutamate
Binding Affinity: -5.2 kcal/mol
F
Glycine overlay with glycine
Binding Affinity: -3.1 kcal/mol
G
Acetic acid overlay with glycine
Binding Affinity: -3.1 kcal/mol

466

467 **Figure 6. Computational modeling of NMDAR binding. (A)** Structure of glutamic acid, acetic
468 acid, glycine, glutaric acid and AP5. **(B)** Computational modeling of glutamate (yellow structure
469 and interactions cyan) overlay in NR1/NR2A NMDAR with native glutamate (green structure and
470 interactions yellow). **(C)** Computational modeling of two acetic acid molecules (cyan structure
471 and interactions red) overlay in NR1/NR2A NMDAR with native glutamate (green structure and
472 interactions yellow). **(D)** Computational modeling of glutaric acid (cyan structure and interactions
473 red) overlay in NR1/NR2A NMDAR with native glutamate (green structure and interactions
474 yellow). **(E)** Computational modeling of AP5 (magenta structure and interactions red) overlay in
475 NR1/NR2A NMDAR with native glutamate (green structure and interactions yellow). **(F)**
476 Computational modeling of glycine (magenta structure and interactions cyan) overlay in
477 NR1/NR2A NMDAR glycine binding pocket with native glycine (green structure and interactions
478 yellow). **(G)** Computational modeling of acetic acid (cyan structure and interactions red) overlay
479 in NR1/NR2A NMDAR glycine binding pocket with native glycine (green structure and
480 interactions yellow).
481

482 **Bath application of acetate induces NMDAR mediated inward currents in CeA-RVLM**
483 **neurons and is not driven by excess extracellular sodium**

484 Next we examined whether external acetate application resulted in NMDAR mediated
485 inward currents in CeA-RVLM neurons. We used memantine as our choice NMDAR antagonist
486 because it showed greater efficacy in our intrinisic excitability protocols. What we found
487 consistent with our excitability study was that bath application of acetate significantly increased
488 NMDAR mediated inward currents, -22.5 ± 2.1 pA (Figure 7). Co-application of acetate and
489 memantine was able to completely abolish NMDAR mediated inward currents, 7.3 ± 5.5 pA

490 (Figure 7). Again, since we were applying acetate as a sodium salt, we wanted to verify that the
491 increased NMDAR mediated inward currents were not due to increased sodium concentration. As
492 such, we used sodium gluconate as a sodium ion control and found that 37.5 mM sodium gluconate
493 was unable to trigger any NMDAR mediated inward currents, -1.1 ± 1.4 pA (Figure 7), suggesting
494 acetate was the bioactive compound.

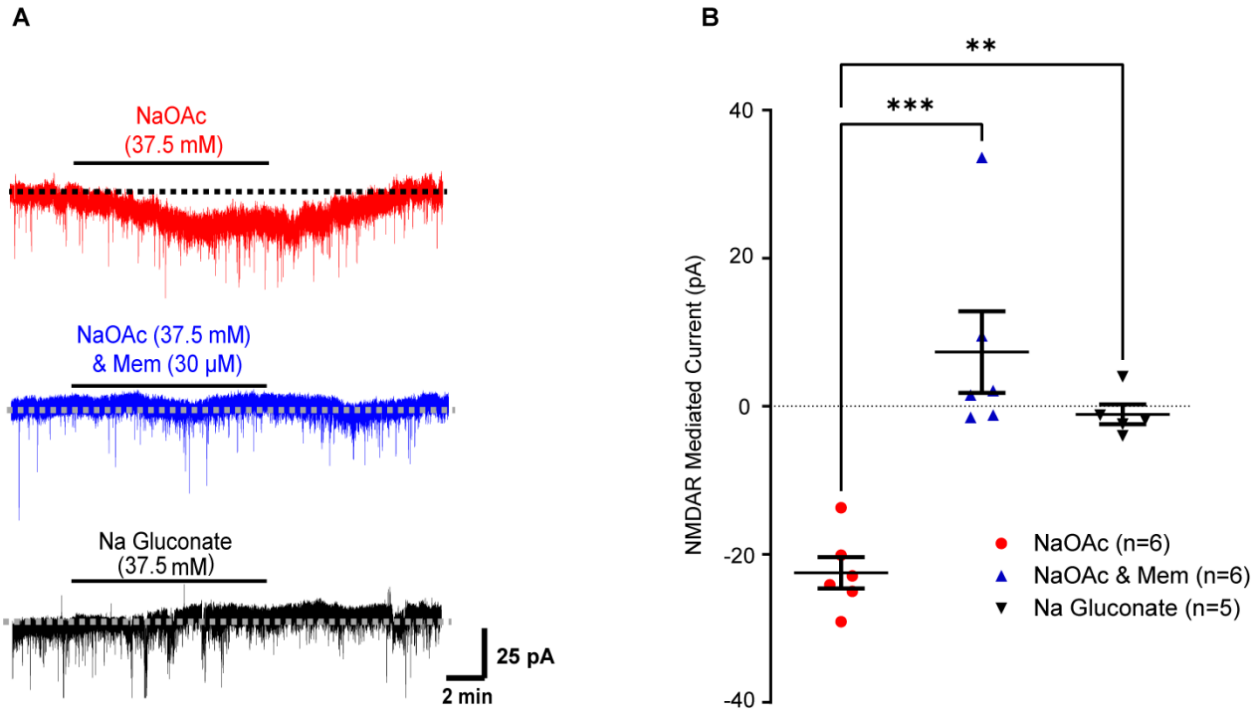

495

496 **Figure 7. Acetate mediated NMDAR currents. (A)** Representative raw traces for NMDAR
497 mediated currents in CeA-RVLM neurons. **(B)** Summary data for NMDAR mediated currents in
498 CeA-RVLM neurons. (***p=0.0001, **p=0.0038) (n=6 neurons, N=4 rats), (n=6 neurons, N=2
499 rats), (n=5 neurons, N=3 rats). Solid black lines above traces denote drug application time followed
500 by washout.

501

502

Bath application of acetate increases depolarizing input resistance (R_{input}) in CeA-RVLM neurons

To further understand the mechanistic effects of external acetate on CeA-RVLM neuronal excitability, neurons were subjected to a ramp protocol aimed to explore voltage threshold for firing an action potential (V_t) and to determine depolarizing input resistance (Depolarizing R_{input}) (Figure 8A-C). Input resistance (impedance) by definition is the measure of the opposition to current in an electrical network (ie, a greater depolarizing R_{input} suggests a greater resistance to positive current injection). Acetate increased the depolariing R_{input} compared to control (0.75 ± 0.04 GΩ vs 0.53 ± 0.05 GΩ) (Figure 8B), but had no statistically significant effect on alterations to V_t (Figure 6D). From an excitability standpoint, increased depolarizing R_{input} suggests an increase of positive ion influx in acetate treated neurons compared to control as they are depolarized. The effect of NMDAR blockers significantly reduced depolarizing R_{input}, ($F_{(3,25)}$ = 4.00, P=0.0186) (Figure 8B).

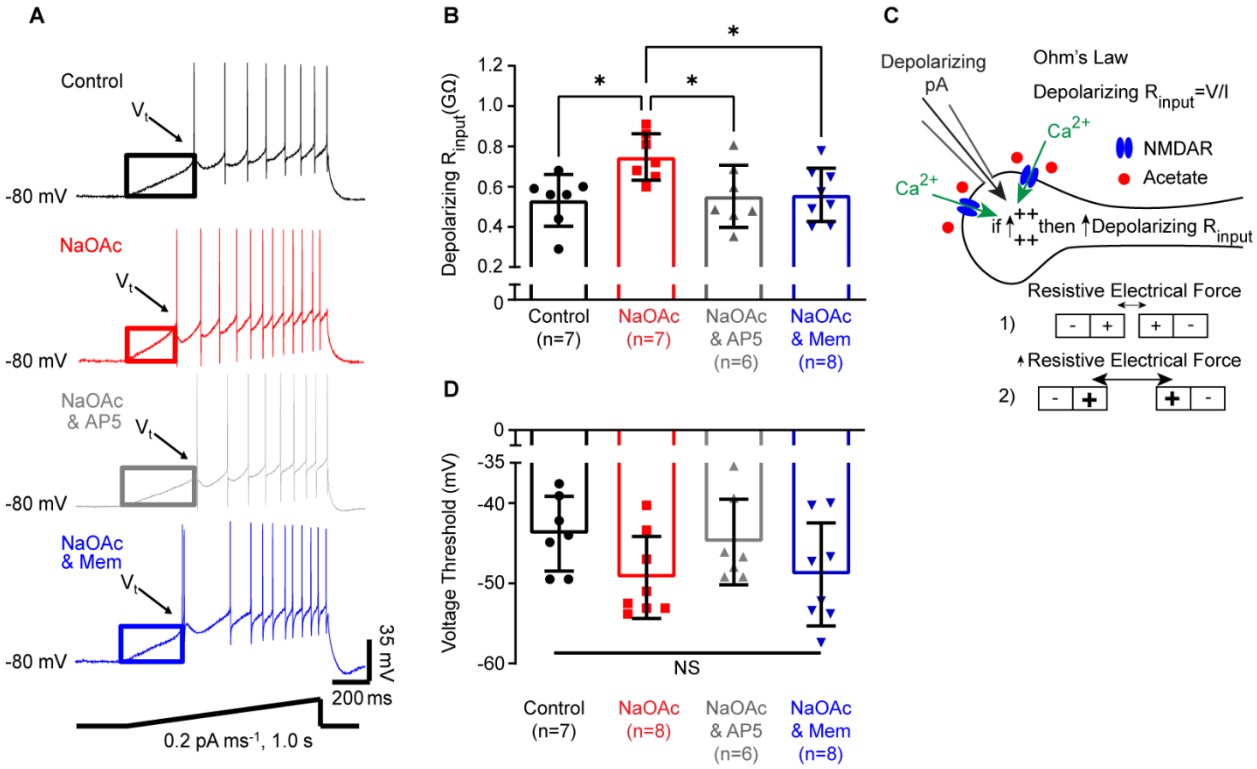

517 **Figure 8. Effect of acetate on depolarizing input resistance (Depolarizing R_{input}) and voltage**
518 **threshold (V_t) to firing an action potential. (A)** Representative raw traces for ramp excitability
519 protocol for control (black), NaOAc (red), NaOAc & AP5 (grey) and NaOAc & memantine (blue).
520 Ramp-current injection protocol below traces. **(B)** Summary data for depolarizing R_{input}. (* $p <$
521 0.05 vs control). **(C)** Graphical summary of depolarizing input resistance. Increased depolarizing
522 current injection and activation of NMDAR results in an increase in positive charge buildup
523 measured as a change in overall resistance via Ohm's law. 1) Baseline electrical charge resistive
524 force, 2) increased calcium enhanced electrical charge resistive force. **(D)** Summary data of voltage
525 threshold to firing an action potential.
526

527 **Bath application of acetate to primary neuronal cultures increases cytosolic calcium and is**
528 **NMDAR dependent**

529 Our lab previously reported that bath application of acetate to dopaminergic-like PC12
530 cells increased cytosolic calcium (14) which was attenuated by co-application of acetate and
531 memantine. We wanted to corroborate our previous findings in primary neuronal cultures. Bath
532 application of acetate (37.5 mM, exact as those used in patch clamp recordings) increased cytosolic
533 calcium fluorescence intensity in primary neurons in a time-dependent manner (baseline, 1 min
534 and 25 min), 3,759 ± 430.5, 6,046 ± 500.7 and 6,775 ± 516.3 CFIT, respectively ($F_{(2,36)} = 10.58$,
535 $p = 0.0002$) (Figure 9 A-C, G). Co-application of acetate (37.5 mM) and memantine (30 μM)
536 completely abolished any acetate induced increase in cytosolic calcium in neurons ($F_{(2,27)} = 0.21$,
537 $p = 0.81$) (Figure 9 D-F, H).

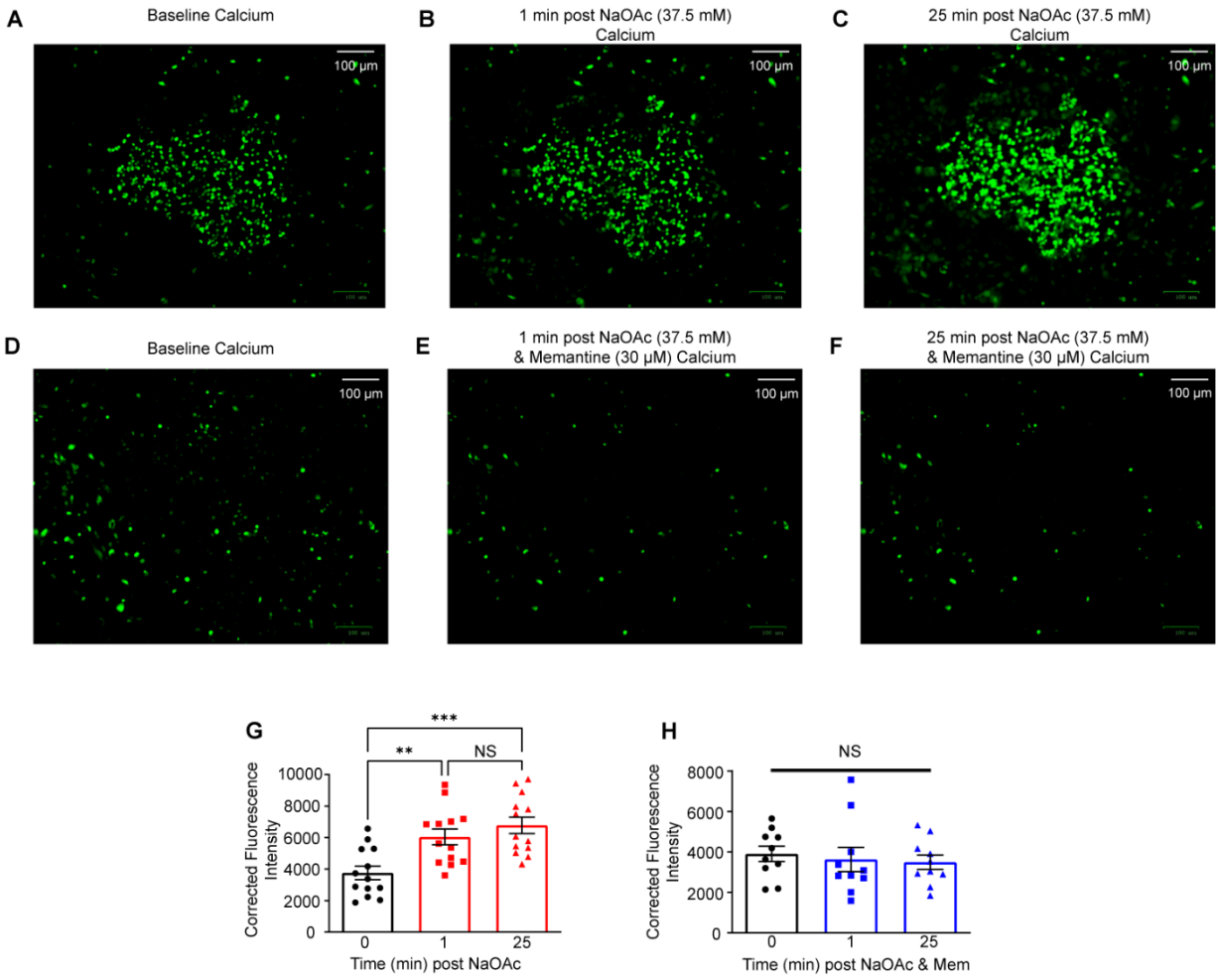

Figure 9. Acetate increases cytosolic calcium in neurons. (A) Baseline calcium fluorescence. **(B)** 1-minute post NaOAc. **(C)** 25 minutes post NaOAc. **(D)** Baseline calcium fluorescence. **(E)** 1-minute post NaOAc & memantine. **(F)** 25 minutes post NaOAc & memantine. **(G)** Neuronal calcium time-course summary data with NaOAc (**p<0.01, ***p<0.001 vs baseline). **(H)** Neuronal calcium time-course summary data with NaOAc & memantine (Mem). Note **A-C** and **D-F** images were acquired from different samples.

549 **DISCUSSION**

550 In the present study, we evaluated how local brain metabolism of ethanol within the CeA
551 elicits sympathoexcitatory responses *in vivo*. We find in a similar fashion to our previously
552 reported work that microinjection of ethanol within the CeA increases SNA and MAP (13).
553 Inhibiting local CeA ethanol metabolism with fomepizole (ADH inhibitor) or cyanamide (ALDH
554 inhibitor) significantly blunts the ethanol induced sympathoexcitatory response. CeA
555 microinjection of the ethanol metabolite, acetate, was found to increase SNA and MAP in a dose-
556 dependent manner. These responses were attenuated by NMDAR antagonists, AP5 or memantine.
557 In brain slice recordings containing CeA autonomic neurons with axon projecting to the RVLM
558 (CeA-RVLM), bath application of acetate dose-dependently increased neuronal excitability with
559 a calculated EC_{50} =5.90 mM and an E_{max} of 37.5 mM. Increased depolarizing input resistance was
560 apparent in acetate treated CeA-RVLM neurons. Co-application of NMDAR antagonists
561 attenuated these acetate induced responses, with memantine proving more effective. Similarly,
562 NMDAR mediated inward currents in the presence of acetate were abolished by co-application
563 with NMDAR antagonist. Finally, in primary neuronal cell cultures, bath application of acetate
564 increased cytosolic calcium in a time-dependent manner, and this response was abolished by co-
565 application of acetate and memantine. These findings suggest that ethanol-mediated inhibition of
566 NMDAR *in vitro* is counteracted by acetate-mediated activation of the same receptor.

567

568 **Ethanol and neural control of cardiovascular function**

569 Human studies have consistently demonstrated that acute ethanol consumption elicits
570 sympathoexcitatory effects (46-48). While these effects are likely a combination of both peripheral
571 and central mechanisms (49), centrally mediated mechanisms remain unclear. Furthermore, only

572 a handful of studies have explored metabolic based mechanisms (13, 50). In our whole-animal
573 SNA recordings from targeted brain delivery, we measure SSNA as well as LSNA. The SSNA
574 closely corresponds with venous blood return and redistribution (51), while LSNA can be inferred
575 as a close proxy for muscle SNA (52). While microinjection of acetate in the CeA increases both
576 SSNA and LSNA, a key finding of increased LSNA may be linked to an effect noted in human
577 studies. Acute ethanol was found to increase muscle SNA in humans (46, 47). Our results of CeA
578 acetate on increased LSNA supports this previously mentioned finding in humans (46, 47),
579 suggesting that increased muscle SNA in humans from ethanol may at least be partially mediated
580 by centrally acting acetate. Future studies investigating the effects of microinjected acetate in other
581 cardiovascular regulatory centers in the brain may delineate diverging, mechanistic and temporal
582 output responses from acetate.
583

584 **Potential active site binding of acetate in NMDAR**

585 Our electrophysiology studies demonstrated differences in the ability of two NMDAR
586 antagonists to blunt the acetate-induced increase in neuronal excitability. We utilized the classic
587 competitive NMDAR antagonist, AP5, and a non-competitive NMDAR pore-blocker, memantine.
588 Our initial hypothesis regarding acetate activation of NMDAR was that the carboxy terminals of
589 glutamate were partially agonized by two acetate molecules within the glutamate binding pocket
590 (Figure 6). While memantine was able to completely abolish the response to acetate, AP5 was only
591 partially effective. This suggests potential competition between AP5 and acetate for the active
592 glutamate site in the NMDAR. We were able to corroborate our experimental findings with
593 computational modeling and docking of glutamic acid, acetic acid and AP5 in the active site of
594 NMDAR. Due to limitations in modeling we were unable to predict the binding affinity for two

595 acetic acid molecules in the glutamate binding pocket. Our compromise was to select a compound
596 with two terminal carboxylic acids and a non-ridgid carbon chain to allow for free rotation about
597 its axis. Glutaric acid, an NMDAR agonist (53, 54), is a five carbon chain molecule with two
598 terminal carboxylic acid functional groups (structurally similar to glutamate with no amine); it
599 displayed higher simulated binding affinity compared to AP5 (-5.4 vs -5.2 kcal/mol), suggesting
600 that two molecules of acetate may outcompete AP5. While we cannot definitively say that acetate
601 actively binds at the glutamate binding pocket in NMDAR, our experimental findings and
602 computational data support this possiblity.

603 We next modeled acetic acid at the glycine binding pocket in the NR1/NR2A NMDAR as
604 acetic acid and glycine also share similar structural homology. Our computational data suggests
605 that acetic acid has similar simulated binding affinity to glycine (-3.1 vs -3.1 kcal/mol). Agonism
606 at the glycine site by acetate may also explain the effectiveness of memantine over AP5 at
607 abolishing acetate-induced neuronal excitability, as glycine has been demonstrated to partially
608 reverse AP5 blockade of NMDAR (55). Taken together, these simulated models suggest that future
609 work investigating the effects of acetate at NMDAR and glycine receptors *in vivo* and *in vitro* are
610 needed.

611

612 **Mechanisms for acetate induced increase in excitability within the CeA**

613 While our present study suggests a major involvement of CeA NMDAR in the acetate
614 induced effects on neuronal excitability and sympathoexcitatory responses, there are other
615 potential contributing mechanisms. Acetate incorporation into glutamatergic (56, 57) as well as
616 GABAergic (2, 40, 56) pools is likely a reflection of astrocytic metabolism. As such, astrocytic
617 influence on glutamate cannot be ruled out. Previous work has demonstrated that acute acetic acid

618 increased mEPSC frequency but not amplitudes, suggesting an increase in presynaptic glutamate
619 (15). Whether this is from astrocytic generation or presynaptic synapses remains to be determined
620 and has yet to be reported in CeA-RVLM neurons.

621 Another potential contribution to increased CeA excitability in the presence of acetate is
622 AMPAR activation. We did see an ethanol induced AMPAR component in our previous
623 microinjection study within the CeA (13), which is likely mediated via metabolism to acetate,
624 however the NMDAR component appeared larger and thus we chose to focus our attention there.
625 However, this AMPAR component may be a contributing factor seen in a lack of apparent
626 effectiveness of AP5 and therefore we cannot rule out the impact of AMPARs in this response,
627 especially as previous studies demonstrate an increase in mEPSC frequencies (likely AMPAR
628 mediated events) in response to acute acetic acid in the accumbens shell (15). The fact that ethanol
629 (44 mM) increased mEPSC frequencies with no apparent effect on intrinsic excitability supports
630 the notion that this linkage to increased intrinsic excitability is not necessarily straightforward
631 given the dissociation between the two (15). Nevertheless, these two previous studies demonstrate
632 an inherent effect of acetic acid/acetate on AMPAR and this contribution deserves more attention
633 in future studies.

634

635 **Perspectives**

636 To the best of our knowledge, we are the first to report the effects of acetate/acetic acid on
637 intrinsic exctiability of neurons, particularly autonomic CeA-RVLM neurons. As such, there is
638 limited availability of literature with which we may compare our findings. Existing literature
639 regarding acetate/acetic acid regulation of neuronal function seems supportive of the notion that
640 both have robust effects in the CNS (2, 40, 58-61) which we also report here. Additionally, to the

641 best of our knowledge there has only been one study describing the effect of ethanol/acetic acid
642 interactions on neurophysiology (15). Future studies of these two pharmacological interactions
643 should be pursued. Furthermore, given that NMDARs are heavily involved in synaptic plasticity
644 (62) and alcohol use disorder (63), our finding that acetic acid/acetate activates NMDAR *in vivo*
645 and *in vitro* may highlight a potential mechanism of alcohol use disorder pathogenesis. More
646 studies are needed to determine the effects of centrally acting acetic acid/acetate on neuronal
647 function and behavioral outputs, including cardiovascular function and whether there are any
648 differences between sexes.
649

650 **Authors' Contribution:**

651 A.D.C., M.J.H., K.M.D., J.E.B. and R.A.L. performed experiments. A.D.C., M.J.H., A.R.C.,
652 K.M.D., J.E.B., R.A.L., Z.S., L.Z. and Q.H.C. analyzed data. A.D.C., A.R.C., Q.H.C. and L.Z.
653 prepared figures. A.D.C., A.R.C., Q.H.C. and L.Z. drafted the manuscript. All authors edited and
654 revised manuscript. All authors approved the final version of the manuscript. A.D.C. and Q.H.C.
655 conceptualized and designed the research.
656

657 **Acknowledgements:**

658 We would like to thank Dr. Timothy W. Chapp and Dr. Scott M. Chapp for their helpful
659 suggestions and proof reading as well as Dr. Joe Erlichman and Dr. Ana Estevez for their early
660 suggestions. The authors also thank Mrs. Mingjun Gu for excellent technical assistance.
661

662 **Sources of funding:**

This study was supported by: NIHR15HL122952 (Chen), NIHR15HL129213 (Shan) and AHA 16PRE27780121 (Chapp).

Disclosures:

None

Table 1. Membrane properties of CeA-RVLM neurons

Group	Neurons (n)	V_m (mV)	C_m (pF)	HR_{input} (GΩ)	V_t (mV)	Rats (n)
Control	7	-58.0 ± 3.0	47.4 ± 2.5	0.47 ± 0.07	-43.8 ± 1.8	5
NaOAc (7.5 mM)	6	-59.5 ± 2.6	45.3 ± 4.5	0.53 ± 0.08	-42.4 ± 2.7	3
NaOAc (37.5 mM)	8	-62.3 ± 2.2	34.6 ± 2.5	0.58 ± 0.03	-49.3 ± 1.8	3
NaOAc (37.5 mM) + AP5 (60 μM)	7	-67.9 ± 4.3	36.3 ± 2.2	0.45 ± 0.07	-45.0 ± 2.5	2
NaOAc (37.5 mM) + Memantine (30 μM)	8	-63.0 ± 3.4	39.0 ± 3.5	0.54 ± 0.10	-47.5 ± 1.7	3
NaOAc (75 mM)	7	-59.9 ± 1.8	42.2 ± 1.6	0.40 ± 0.04	-47.7 ± 1.1	3

669 Values are mean ± SEM; n = number size, V_m resting membrane potential, C_m capacitance, HR_{input}
670 hyperpolarizing input resistance, V_t voltage threshold for action potential, NaOAc sodium acetate.

671

672

673

674

675 **REFERENCES**

676

677 1. **Wang J, Du H, Jiang L, Ma X, de Graaf RA, Behar KL, and Mason GF**. Oxidation of ethanol
678 in the rat brain and effects associated with chronic ethanol exposure. *Proc Natl Acad Sci U S A* 110: 14444-
679 14449, 2013.
680 2. **Jiang L, Gulanski BI, De Feyter HM, Weinzimer SA, Pittman B, Guidone E, Koretski J,**
681 **Harman S, Petrakis IL, Krystal JH, and Mason GF**. Increased brain uptake and oxidation of acetate in
682 heavy drinkers. *J Clin Invest* 123: 1605-1614, 2013.
683 3. **Brodie MS, Pesold C, and Appel SB**. Ethanol directly excites dopaminergic ventral tegmental
684 area reward neurons. *Alcoholism, clinical and experimental research* 23: 1848-1852, 1999.
685 4. **Lovinger DM, White G, and Weight FF**. Ethanol inhibits NMDA-activated ion current in
686 hippocampal neurons. *Science* 243: 1721-1724, 1989.
687 5. **Lovinger D, White G, and Weight F**. NMDA receptor-mediated synaptic excitation selectively
688 inhibited by ethanol in hippocampal slice from adult rat. *The Journal of Neuroscience* 10: 1372-1379, 1990.
689 6. **Grover CA, Frye GD, and Griffith WH**. Acute tolerance to ethanol inhibition of NMDA-
690 mediated EPSPs in the CA1 region of the rat hippocampus. *Brain Research* 642: 70-76, 1994.
691 7. **Hicklin TR, Wu PH, Radcliffe RA, Freund RK, Goebel-Goody SM, Correa PR, Proctor WR,**
692 **Lombroso PJ, and Browning MD**. Alcohol inhibition of the NMDA receptor function, long-term
693 potentiation, and fear learning requires striatal-enriched protein tyrosine phosphatase. *Proceedings of the*
694 *National Academy of Sciences* 108: 6650-6655, 2011.
695 8. **Karkhanis AN, Huggins KN, Rose JH, and Jones SR**. Switch from excitatory to inhibitory
696 actions of ethanol on dopamine levels after chronic exposure: Role of kappa opioid receptors.
697 *Neuropharmacology* 110: 190-197, 2016.
698 9. **Roh MS, Cui FJ, Kim HK, and Kang UG**. Regulation of NMDA receptor subunits after acute
699 ethanol treatment in rat brain. *Alcohol and alcoholism (Oxford, Oxfordshire)* 46: 672-679, 2011.
700 10. **Karadayian AG, Malanga G, Czerniczyniec A, Lombardi P, Bustamante J, and Lores-Arnaiz**
701 **S**. Free radical production and antioxidant status in brain cortex non-synaptic mitochondria and
702 synaptosomes at alcohol hangover onset. *Free radical biology & medicine* 108: 692-703, 2017.
703 11. **Wiese JG, Shlipak MG, and Browner WS**. The Alcohol Hangover. *Annals of Internal Medicine*
704 132: 897-902, 2000.
705 12. **Maxwell CR, Spangenberg RJ, Hoek JB, Silberstein SD, and Oshinsky ML**. Acetate Causes
706 Alcohol Hangover Headache in Rats. *PLoS ONE* 5: e15963, 2010.
707 13. **Chapp AD, Gui L, Huber MJ, Liu J, Larson RA, Zhu J, Carter JR, and Chen QH**.
708 Sympathoexcitation and pressor responses induced by ethanol in the central nucleus of amygdala involves
709 activation of NMDA receptors in rats. *Am J Physiol Heart Circ Physiol* 307: H701-709, 2014.
710 14. **Chapp AD, Behnke JE, Driscoll KM, Fan Y, Hoban E, Shan Z, Zhang L, and Chen QH**.
711 Acetate Mediates Alcohol Excitotoxicity in Dopaminergic-like PC12 Cells. *ACS Chem Neurosci* 10: 235-
712 245, 2019.
713 15. **Chapp AD, Mermelstein PG, and Thomas MJ**. The Ethanol Metabolite Acetic Acid Activates

714 Mouse Nucleus Accumbens Shell Medium Spiny Neurons. *J Neurophysiol* 2021.
715 16. **Gui L, LaGrange LP, Larson RA, Gu M, Zhu J, and Chen QH**. Role of small conductance
716 calcium-activated potassium channels expressed in PVN in regulating sympathetic nerve activity and
717 arterial blood pressure in rats. *Am J Physiol Regul Integr Comp Physiol* 303: R301-310, 2012.
718 17. **Stocker SD, and Muntzel MS**. Recording sympathetic nerve activity chronically in rats: surgery
719 techniques, assessment of nerve activity, and quantification. *American journal of physiology Heart and*
720 *circulatory physiology* 305: H1407-1416, 2013.
721 18. **Chen QH, Haywood JR, and Toney GM**. Sympathoexcitation by PVN-injected bicuculline
722 requires activation of excitatory amino acid receptors. *Hypertension* 42: 725-731, 2003.
723 19. **Chen QH, and Toney GM**. Excitability of paraventricular nucleus neurones that project to the
724 rostral ventrolateral medulla is regulated by small-conductance Ca2+-activated K+ channels. *J Physiol* 587:
725 4235-4247, 2009.
726 20. **Shan Z, Shi P, Cuadra AE, Dong Y, Lamont GJ, Li Q, Seth DM, Navar LG, Katovich MJ,**
727 **Sumners C, and Raizada MK**. Involvement of the brain (pro)renin receptor in cardiovascular homeostasis.
728 *Circulation research* 107: 934-938, 2010.
729 21. **Chapp AD, Behnke JE, Driscoll KM, Hahka T, LaLonde Z, Shan Z, and Chen QH**. Elevated
730 L-lactate Promotes Major Cellular Pathologies Associated with Neurodegenerative Diseases. *Neurosci Bull*
731 2020.
732 22. **Schneider CA, Rasband WS, and Eliceiri KW**. NIH Image to ImageJ: 25 years of image analysis.
733 *Nature methods* 9: 671-675, 2012.
734 23. **Knight CP, Hauser SR, Waeiss RA, Molosh AI, Johnson PL, Truitt WA, McBride WJ, Bell**
735 **RL, Shekhar A, and Rodd ZA**. The Rewarding and Anxiolytic Properties of Ethanol within the Central
736 Nucleus of the Amygdala: Mediated by Genetic Background and Nociceptin. *J Pharmacol Exp Ther* 374:
737 366-375, 2020.
738 24. **Pardo M, Betz AJ, San Miguel N, López-Cruz L, Salamone JD, and Correa M**. Acetate as an
739 active metabolite of ethanol: studies of locomotion, loss of righting reflex, and anxiety in rodents. *Front*
740 *Behav Neurosci* 7: 81, 2013.
741 25. **Cederbaum AI**. Alcohol metabolism. *Clin Liver Dis* 16: 667-685, 2012.
742 26. **Furukawa H, Singh SK, Mancusso R, and Gouaux E**. Subunit arrangement and function in
743 NMDA receptors. *Nature* 438: 185-192, 2005.
744 27. **Dallakyan S, and Olson AJ**. Small-molecule library screening by docking with PyRx. *Methods*
745 *Mol Biol* 1263: 243-250, 2015.
746 28. **Schrödinger L**. The PyMOL Molecular Graphics System, Version 2.0
747 29. **Sarkola T, Iles MR, Kohlenberg-Mueller K, and Eriksson CJ**. Ethanol, acetaldehyde, acetate,
748 and lactate levels after alcohol intake in white men and women: effect of 4-methylpyrazole. *Alcohol Clin*
749 *Exp Res* 26: 239-245, 2002.
750 30. **Demaster EG, Nagasawa HT, and Shirota FN**. Metabolic activation of cyanamide to an inhibitor
751 of aldehyde dehydrogenase in vitro. *Pharmacology, biochemistry, and behavior* 18 Suppl 1: 273-277, 1983.
752 31. **Alaux-Cantin S, Buttolo R, Houchi H, Jeanblanc J, and Naassila M**. Memantine reduces
753 alcohol drinking but not relapse in alcohol-dependent rats. *Addiction biology* 2014.
754 32. **Idrus NM, McGough NN, Riley EP, and Thomas JD**. Administration of memantine during
755 withdrawal mitigates overactivity and spatial learning impairments associated with neonatal alcohol
756 exposure in rats. *Alcoholism, clinical and experimental research* 38: 529-537, 2014.
757 33. **Zhou X, Hollern D, Liao J, Andrechek E, and Wang H**. NMDA receptor-mediated excitotoxicity
758 depends on the coactivation of synaptic and extrasynaptic receptors. *Cell Death Dis* 4: e560, 2013.
759 34. **van Marum RJ**. Update on the use of memantine in Alzheimer's disease. *Neuropsychiatric*
760 *Disease and Treatment* 5: 237-247, 2009.
761 35. **Bisaga A, and Evans SM**. Acute effects of memantine in combination with alcohol in moderate
762 drinkers. *Psychopharmacology* 172: 16-24, 2004.
763 36. **Olney JW, Labruyere J, and Price MT**. Pathological changes induced in cerebrocortical neurons
764 by phencyclidine and related drugs. *Science* 244: 1360-1362, 1989.

37. **Gershman H, and Steeper J**. Rate of clearance of ethanol from the blood of intoxicated patients in the emergency department. *J Emerg Med* 9: 307-311, 1991.
38. **Roberto M, Madamba SG, Stouffer DG, Parsons LH, and Siggins GR**. Increased GABA Release in the Central Amygdala of Ethanol-Dependent Rats. *The Journal of Neuroscience* 24: 10159-10166, 2004.
39. **Roberts JR, and Dollard D**. Alcohol Levels Do Not Accurately Predict Physical or Mental Impairment in Ethanol-Tolerant Subjects: Relevance to Emergency Medicine and Dram Shop Laws. *Journal of Medical Toxicology* 6: 438-442, 2010.
40. **Jin S, Cao Q, Yang F, Zhu H, Xu S, Chen Q, Wang Z, Lin Y, Cinar R, Pawlosky RJ, Zhang Y, Xiong W, Gao B, Koob GF, Lovinger DM, and Zhang L**. Brain ethanol metabolism by astrocytic ALDH2 drives the behavioural effects of ethanol intoxication. *Nature Metabolism* 3: 337-351, 2021.
41. **Davies DL, Crawford DK, Trudell JR, Mihic SJ, and Alkana RL**. Multiple sites of ethanol action in alpha1 and alpha2 glycine receptors suggested by sensitivity to pressure antagonism. *J Neurochem* 89: 1175-1185, 2004.
42. **Valenzuela CF, Cardoso RA, Wick MJ, Weiner JL, Dunwiddie TV, and Harris RA**. Effects of ethanol on recombinant glycine receptors expressed in mammalian cell lines. *Alcohol Clin Exp Res* 22: 1132-1136, 1998.
43. **Nakahiro M, Arakawa O, and Narahashi T**. Modulation of gamma-aminobutyric acid receptor-channel complex by alcohols. *J Pharmacol Exp Ther* 259: 235-240, 1991.
44. **Chen Q-H, and Toney GM**. In Vivo Discharge Properties of Hypothalamic Paraventricular Nucleus Neurons With Axonal Projections to the Rostral Ventrolateral Medulla. *Journal of Neurophysiology* 103: 4-15, 2010.
45. **Lin JC, Tsao WL, and Wang Y**. Cardiovascular effects of NMDA in the RVLM of spontaneously hypertensive rats. *Brain Research Bulletin* 37: 289-294, 1995.
46. **Carter JR, Stream SF, Durocher JJ, and Larson RA**. Influence of acute alcohol ingestion on sympathetic neural responses to orthostatic stress in humans. *American Journal of Physiology-Endocrinology and Metabolism* 300: E771-E778, 2011.
47. **Randin D, Vollenweider P, Tappy L, Jéquier E, Nicod P, and Scherrer U**. Suppression of Alcohol-Induced Hypertension by Dexamethasone. *New England Journal of Medicine* 332: 1733-1738, 1995.
48. **Greenlund IM, Cunningham HA, Tikkanen AL, Bigalke JA, Smoot CA, Durocher JJ, and Carter JR**. Morning sympathetic activity after evening binge alcohol consumption. *American Journal of Physiology-Heart and Circulatory Physiology* 320: H305-H315, 2021.
49. **Husain K, Ansari RA, and Ferder L**. Alcohol-induced hypertension: Mechanism and prevention. *World J Cardiol* 6: 245-252, 2014.
50. **El-Mas MM, and Abdel-Rahman AA**. Enhanced catabolism to acetaldehyde in rostral ventrolateral medullary neurons accounts for the pressor effect of ethanol in spontaneously hypertensive rats. *American journal of physiology Heart and circulatory physiology* 302: H837-H844, 2012.
51. **Fudim M, Yalamuri S, Herbert JT, Liu PR, Patel MR, and Sandler A**. Raising the pressure: Hemodynamic effects of splanchnic nerve stimulation. *J Appl Physiol (1985)* 123: 126-127, 2017.
52. **Miki K, Oda M, Kamijyo N, Kawahara K, and Yoshimoto M**. Lumbar sympathetic nerve activity and hindquarter blood flow during REM sleep in rats. *The Journal of physiology* 557: 261-271, 2004.
53. **Tian F, Fu X, Gao J, Ying Y, Hou L, Liang Y, Ning Q, and Luo X**. Glutaric Acid-Mediated Apoptosis in Primary Striatal Neurons. *BioMed Research International* 2014: 484731, 2014.
54. **Kölker S, Ahlemeyer B, Krieglstein J, and Hoffmann GF**. 3-Hydroxyglutaric and glutaric acids are neurotoxic through NMDA receptors in vitro. *J Inherit Metab Dis* 22: 259-262, 1999.
55. **Minota S, Miyazaki T, Wang MY, Read HL, and Dun NJ**. Glycine potentiates NMDA responses in rat hippocampal CA1 neurons. *Neurosci Lett* 100: 237-242, 1989.
56. **Rae C, Fekete AD, Kashem MA, Nasrallah FA, and Bröer S**. Metabolism, compartmentation, transport and production of acetate in the cortical brain tissue slice. *Neurochem Res* 37: 2541-2553, 2012.

57. **Frost G, Sleeth ML, Sahuri-Arisoylu M, Lizarbe B, Cerdan S, Brody L, Anastasovska J, Ghourab S, Hankir M, Zhang S, Carling D, Swann JR, Gibson G, Viardot A, Morrison D, Louise Thomas E, and Bell JD**. The short-chain fatty acid acetate reduces appetite via a central homeostatic mechanism. *Nat Commun* 5: 3611, 2014.
58. **Drapeau P, and Nachshen DA**. Effects of lowering extracellular and cytosolic pH on calcium fluxes, cytosolic calcium levels, and transmitter release in presynaptic nerve terminals isolated from rat brain. *J Gen Physiol* 91: 305-315, 1988.
59. **Frost G, Sleeth ML, Sahuri-Arisoylu M, Lizarbe B, Cerdan S, Brody L, Anastasovska J, Ghourab S, Hankir M, Zhang S, Carling D, Swann JR, Gibson G, Viardot A, Morrison D, Louise Thomas E, and Bell JD**. The short-chain fatty acid acetate reduces appetite via a central homeostatic mechanism. *Nat Commun* 5: 2014.
60. **Perry RJ, Peng L, Barry NA, Cline GW, Zhang D, Cardone RL, Petersen KF, Kibbey RG, Goodman AL, and Shulman GI**. Acetate mediates a microbiome-brain-beta-cell axis to promote metabolic syndrome. *Nature* 534: 213-217, 2016.
61. **Chen Y-H, Wu M-L, and Fu W-M**. Regulation of Presynaptic NMDA Responses by External and Intracellular pH Changes at Developing Neuromuscular Synapses. *The Journal of Neuroscience* 18: 2982-2990, 1998.
62. **Paoletti P, Bellone C, and Zhou Q**. NMDA receptor subunit diversity: impact on receptor properties, synaptic plasticity and disease. *Nat Rev Neurosci* 14: 383-400, 2013.
63. **Ron D, and Wang J**. Frontiers in Neuroscience. The NMDA Receptor and Alcohol Addiction. In: *Biology of the NMDA Receptor*, edited by Van Dongen AM. Boca Raton (FL): CRC Press/Taylor & Francis Copyright © 2009, Taylor & Francis Group, LLC., 2009.